Realized SemiCovariances: Looking for Signs of Direction Inside the Covariance Matrix

This version: September 22, 2017

Tim Bollerslev[a,*], Andrew J. Patton[b], Rogier Quaedvlieg[c]

[a] *Department of Economics, Duke University, NBER and CREATES*
[b] *Department of Economics, Duke University*
[c] *Erasmus School of Economics, Erasmus University Rotterdam*

Abstract

We propose a new decomposition of the realized covariance matrix into four "realized semicovariance" components based on the signs of the underlying high-frequency returns. We derive the asymptotic distribution for the different components under the assumption of a continuous multivariate semimartingale and standard infill asymptotic arguments. Based on high-frequency returns for a large cross-section of individual stocks, we document distinctly different features and dynamic dependencies in the different semicovariance components. We demonstrate that the accuracy of portfolio return variance forecasts may be significantly improved by exploiting these differences and "looking inside" the realized covariance matrices for signs of direction.

Keywords: High-frequency data; realized variances; semicovariances; asymmetric correlations; cojumps; volatility forecasting.
JEL: C22, C51, C53, C58

[☆] We would like to thank Fulvio Corsi, Jia Li, and seminar participants at the University of Padova, Ca'Foscari University of Venice, and the 2017 conferences on "Big Data in Predictive Dynamic Econometric Modeling" at the University of Pennsylvania and "Financial Econometrics" at Boston University for helpful comments. We would also like to thank Bingzhi Zhao for kindly providing us with the cleaned high-frequency data underlying our empirical investigations.

[*] Corresponding author: Department of Economics, Duke University, 213 Social Sciences Building, Box 90097, Durham, NC 27708-0097, United States. Email: boller@duke.edu. The supplemental appendix to this paper is available at http://www.econ.duke.edu/∼boller/research.html.

1. Introduction

The covariance matrix of asset returns is a crucial input to portfolio and risk management decisions. There is a substantial literature on the practical estimation, modeling, and prediction of these covariance matrices dating back more than half a century (e.g., Kendall (1953), Elton and Gruber (1973), and Bauwens, Laurent, and Rombouts (2006)). More recent developments have included the use of high-frequency data for more reliable estimation of lower-frequency realized return covariances (e.g., Andersen, Bollerlsev, Diebold, and Labys (2003), Barndorff-Nielsen and Shephard (2004a), and Barndorff-Nielsen, Hansen, Lunde, and Shephard (2011)); new methods for capturing dynamics in conditional covariance matrices (e.g., Engle (2002) and Bollerslev, Patton, and Quaedvlieg (2016)); and the estimation of covariance matrices in "vast" dimensions (e.g., Fan, Li, and Yu (2012), Hautsch, Kyj, and Malec (2015), and Aït-Sahalia and Xiu (2015)).

Building on this existing literature, we propose a new decomposition of the realized covariance matrix into four unique additive "realized semicovariance" components depending upon the signs of the underlying high-frequency returns. The realized semicovariance matrices may be seen as a high-frequency based multivariate extension of semivariances, which have a long history in finance (e.g., Markowitz (1959), Mao (1970), Hogan and Warren (1972, 1974), and Fishburn (1977)).[1] They also naturally extend the realized semivariances originally proposed by Barndorff-Nielsen, Kinnebrock, and Shephard (2010) to a multivariate context.

We derive the limiting distribution of the new realized semicovariance matrices under the assumption of a continuous multivariate semimartingale and standard infill asymptotics. A small Monte Carlo simulation experiment corroborates the reliability of our asymptotic approximations. In addition to establishing the theoretical properties of the realized semicovariance matrices, we employ high-frequency data for a large cross-section U.S. equities spanning more than a decade to cast light on their empirical properties.

We find that the realized semicovariances have different dynamic dependencies from the usual realized covariances, with the semicovariances based on discordant returns (i.e., returns of opposite signs) exhibiting the strongest memory. These differences in the persistence of the different semicovariance components suggest

[1] Hogan and Warren (1974), in particular, first introduced the notion of the gains "cosemivariance" which is related to, though distinctly different from, the semicovariances we propose here.

that they may contain additional useful information about asset return dependencies over and above that embedded in the usual covariance matrix. Corroborating this idea, we find that out-of-sample forecasts of portfolio return variances may be significantly improved relative to existing procedures that "only" rely on realized variances (e.g., Corsi, 2009) or realized semivariances (e.g., Patton and Sheppard, 2015), by "looking inside" the covariance matrix and separately utilizing the new semicovariance measures. Moreover, the relative gains from doing so increase monotonically with the dimension of the portfolio, although in line with the gains from naïve diversification they also tend to reach somewhat of an asymptote for increasingly large portfolios.[2]

The improved forecasting performance of models based on the new semicovariance measures may be attributed to the different information content that reside in the different components. This is naturally linked to work on the asymmetric reaction of volatility and covariances to news (e.g., Kroner and Ng (1998) and Cappiello, Engle, and Sheppard (2006)). Alternatively, the forecast improvements may be understood by interpreting the semicovariance-based models as time-varying parameter versions of conventional models. Using this interpretation, the semicovariance-based models place substantially more weight on more recent information than conventional models, thereby allowing the models to react more quickly to new information. Interestingly, while the erratic nature of volatility during the financial crisis typically leads conventional volatility forecasting models to reduce the weight on recent observations, the semicovariance-based models actually *increase* the weight, primarily due to an increase in the short-run importance of the negative semicovariance component.

Our asymptotic distributional results also facilitate the construction of tests of hypotheses involving the semicovariance components. For example, one might test whether the realized semicovariances for pairwise positive returns are equal to the semicovariances for pairwise negative returns, a hypothesis we find strong evidence against in our data. These tests are related to asymmetric dependence tests that have appeared in the literature (e.g., Longin and Solnik (2001), Ang and Chen (2002) and Hong, Tu, and Zhou (2007)). They are also related to empirical work on the correlations between asset returns in "bear" and "bull" markets and asymmetric tail dependencies (e.g., Patton (2004), Poon, Rockinger, and Tawn (2004), and Tjøsthem and Hufthammer (2013)), as well as recent work on high-frequency based empirical measures of co-skewness and co-kurtosis (e.g.,

[2]Similar gains may naturally be obtained for forecasts of multivariate covariance matrices; these additional results are reported in the Supplemental Appendix.

Neuberger (2012) and Amaya, Christoffersen, Jacobs, and Vasquez (2015)), and jumps and co-jumps (e.g., Das and Uppal (2004), Bollerslev, Law, and Tauchen (2008), Lee and Mykland (2008), Mancini and Gobbi (2012), Jacod and Todorov (2009), and Li, Todorov, and Tauchen (2017)). In contrast to these existing studies, we retain the covariance matrix as the summary measure of dependence, and instead use information from "bull," "bear" and "mixed" high-frequency returns to "look inside" the realized covariance matrix as way to reveal additional information about the inherent dependencies.

The remainder of the paper is organized as follows. Section 2 formally defines the realized semicovariance measures, derives their asymptotic properties, and presents simulation results on their finite-sample behavior. Section 3 discusses the empirical properties of realized semicovariances based on high-frequency data for more than seven hundred U.S. equities over the period 1993 to 2014. Section 4 concludes. A technical Appendix contains all proofs, and a Supplemental Appendix contains additional empirical results.

2. Realized Semicovariances

Our decomposition of the realized covariance matrix into its four unique "realized semicovariance" components parallels the decomposition of the realized variance into its two unique realized semivariance components.

2.1. Definitions and Basic Properties

To set out the main idea, let $r_{t,k,i}$ denote the return over the k^{th} intradaily time on day t for asset i. Further, denote the corresponding $N \times 1$ vector of returns, over equally-spaced intra-daily intervals, for the set of N assets by $\mathbf{r}_{t,k} \equiv [r_{t,k,1}, ..., r_{t,k,N}]'$. The standard $N \times N$ daily realized covariance matrix is then defined by the summation,

$$\mathbf{RCOV}_t^{(m)} \equiv \sum_{k=1}^{m} \mathbf{r}_{t,k}\mathbf{r}_{t,k}', \tag{1}$$

where m signifies the total number of intradaily return observations available per day.

Now define the $N \times 1$ vectors of signed high-frequency returns,

$$\mathbf{r}_{t,k}^{+} \equiv \mathbf{r}_{t,k} \odot \mathbf{1}, \{\mathbf{r}_{t,k} > 0\}, \tag{2}$$

$$\mathbf{r}_{t,k}^{-} \equiv \mathbf{r}_{t,k} \odot \mathbf{1}, \{\mathbf{r}_{t,k} \leq 0\}, \tag{3}$$

where $\mathbf{1}\{\mathbf{r}_{t,k} > 0\} \equiv [\mathbf{1}\{r_{t,k,1} > 0\}, ..., \mathbf{1}\{r_{t,k,N} > 0\}]'$ denotes the element-wise indicator function equal to 0 or 1 depending on the sign of the k^{th} intradaily return for each of the N assets, with $\mathbf{1}\{\mathbf{r}_{t,k} \leq 0\}$ defined analogously. The standard realized covariance matrix may then be decomposed into four separate "realized semicovariance matrices,"

$$\begin{aligned} \mathbf{P}_t^{(m)} &\equiv \sum_{k=1}^{m} \mathbf{r}_{t,k}^{+} \, \mathbf{r}_{t,k}^{+\prime}, \qquad \mathbf{M}_t^{(m)+} \equiv \sum_{k=1}^{m} \mathbf{r}_{t,k}^{+} \, \mathbf{r}_{t,k}^{-\prime}, \\ \mathbf{M}_t^{(m)-} &\equiv \sum_{k=1}^{m} \mathbf{r}_{t,k}^{-} \, \mathbf{r}_{t,k}^{+\prime}, \qquad \mathbf{N}_t^{(m)} \equiv \sum_{k=1}^{m} \mathbf{r}_{t,k}^{-} \, \mathbf{r}_{t,k}^{-\prime}, \end{aligned} \tag{4}$$

where $\mathbf{P}$, $\mathbf{N}$, and $\mathbf{M}$ stand for "positive," "negative," and "mixed," respectively, referring to the signs of the underlying return vectors. It follows readily that,

$$\mathbf{RCOV}_t^{(m)} = \mathbf{P}_t^{(m)} + \mathbf{N}_t^{(m)} + \mathbf{M}_t^{(m)+} + \mathbf{M}_t^{(m)-}, \tag{5}$$

for all m. Since $\mathbf{RCOV}_t^{(m)}$, $\mathbf{P}_t^{(m)}$, and $\mathbf{N}_t^{(m)}$ are all defined as sums of vector outer-products, these matrices are all positive semidefinite. On the other hand, since the diagonal elements of $\mathbf{M}_t^{(m)+}$ and $\mathbf{M}_t^{(m)-}$ are identically zero by construction, these matrices are necessarily indefinite.[3]

In some applications there is a clear ordering of the assets, endowing the $\mathbf{M}_t^{(m)+}$ and $\mathbf{M}_t^{(m)-}$ realized semicovariances with different economic interpretations.[4] In other situations, the ordering of the assets is arbitrary, and one might expect $\mathbf{M}_t^{(m)+}$ and $\mathbf{M}_t^{(m)-}$ to convey the same information. In those situations the two mixed terms are naturally combined into a single realized semicovariance matrix,

$$\mathbf{M}_t^{(m)} \equiv \mathbf{M}_t^{(m)+} + \mathbf{M}_t^{(m)-}, \tag{6}$$

thus decomposing the standard realized covariance matrix into just three terms, the positive, negative, and mixed realized semicovariances: $\mathbf{P}_t^{(m)}$, $\mathbf{N}_t^{(m)}$, and $\mathbf{M}_t^{(m)}$.

The diagonal elements of $\mathbf{P}_t^{(m)}$ and $\mathbf{N}_t^{(m)}$ correspond to the positive and negative realized semivariances for each of the $i = 1, 2, ..., N$ assets, denoted $\mathcal{V}_{i,t}^{(m)+}$ and $\mathcal{V}_{i,t}^{(m)-}$ respectively. The off-diagonal elements of these (symmetric) matrices correspond to the positive, negative realized semi*co*variances, and we denote the

[3]This means that while the positive and negative "realized semicorrelation" matrices are straightforwardly defined, the "mixed" case is not. We focus on realized semicovariance matrices in this paper.

[4]For example, if one of the assets is an aggregate market portfolio, while the remaining $N-1$ assets are individual stocks, the interpretation of the elements in $\mathbf{M}_t^{(m)+}$ and $\mathbf{M}_t^{(m)-}$ will naturally differ.

(i,j) elements of these matrices (for $i \neq j$) as $\mathcal{P}_{ij,t}^{(m)}$ and $\mathcal{N}_{ij,t}^{(m)}$. In particular, for $N = 2$,

$$\mathbf{P}_t^{(m)} = \begin{bmatrix} \mathcal{V}_{1,t}^{(m)+} & \mathcal{P}_{12,t}^{(m)} \\ \bullet & \mathcal{V}_{2,t}^{(m)+} \end{bmatrix}, \ \mathbf{N}_t^{(m)} = \begin{bmatrix} \mathcal{V}_{1,t}^{(m)-} & \mathcal{N}_{12,t}^{(m)} \\ \bullet & \mathcal{V}_{2,t}^{(m)-} \end{bmatrix}, \ \mathbf{M}_t^{(m)} = \begin{bmatrix} 0 & \mathcal{M}_{12,t}^{(m)} \\ \bullet & 0 \end{bmatrix}. \tag{7}$$

For simplicity, we will drop the "ij" subscripts on $\mathcal{P}_t^{(m)}$, $\mathcal{N}_t^{(m)}$, and $\mathcal{M}_t^{(m)}$ when they are not needed. Equation (7) emphasizes that the novel components of the realized semicovariance matrices proposed here are their off-diagonal elements. These elements contain different, potentially richer, information to that afforded by the decomposition of variances into semivariances.

To illustrate, Figure 1 plots the off-diagonal elements of the daily realized semicovariance matrices averaged across 500 randomly-selected pairs of S&P 500 stocks over the 1993–2014 period.[5] The mixed $\mathcal{M}_t$ component is, of course, always negative, while $\mathcal{P}_t + \mathcal{N}_t$ is always positive. The "concordant" $(\mathcal{P}_t + \mathcal{N}_t)$ and "discordant" $(\mathcal{M}_t)$ terms are typically fairly similar in magnitude. In periods of high volatility, however, $\mathcal{P}_t + \mathcal{N}_t$ increases substantially more than $\mathcal{M}_t$ declines, in line with the widely held belief that during periods of financial market stress correlations and tail dependencies among most financial assets tend to increase. Correspondingly, the off-diagonal element of $\mathbf{RCOV}_t$ (denoted $RCOV_t$) is almost exclusively determined by the two concordant realized semicovariance components in high volatility periods. Further corroborating the idea that the concordant semicovariances are related to notions of market stress, we find that the average correlation of $\mathcal{P}_t$ and $\mathcal{N}_t$ with the VIX volatility index, popularly interpreted as a market "fear gauge," equal 0.484 and 0.477, respectively, compared to 0.285 for $RCOV_t$.

To provide some intuition for the new measures, consider the case of $m = 1$; i.e., using only one return per day. (For notational simplicity below, we suppress the dependence on m.) Further assume that the daily returns are normally distributed with zero mean, unit variance, and cross-asset correlation ρ, so that the expected covariation equals,

$$\mathbb{E}(\mathbf{RCOV}_t) \ = \ \mathbf{I}_N \ + \ (\mathbf{J}_N - \mathbf{I}_N)\rho, \tag{8}$$

where $\mathbf{I}_N$ denotes the $N \times N$ identity matrix, and $\mathbf{J}_N$ is an $N \times N$ matrix of ones.

[5] More detailed descriptions of the data and the procedures used in calculating the realized semicovariances are provided in Section 3.1 below. To avoid cluttering the figure, we combine $\mathcal{P}_t$ and $\mathcal{N}_t$ into a single term, and smooth the daily measures using a $[t-25 : t+25]$ moving average.

Figure 1: *RCOV* decomposition

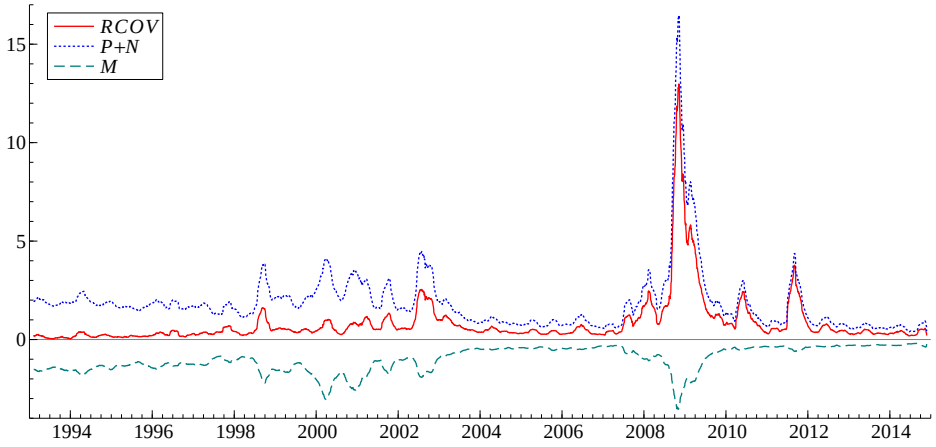

Note: The figure plots the (smoothed) daily realized semicovariances averaged across 1,000 random pairs of S&P 500 stocks over the 1993–2014 period.

It follows then by standard arguments pertaining to the normal distribution[6] that,

$$\mathbb{E}(\mathbf{P}_t) \;=\; \mathbb{E}(\mathbf{N}_t) \;=\; \frac{1}{2}\mathbf{I}_N \;+\; (\mathbf{J}_N - \mathbf{I}_N) \times \frac{\sqrt{1-\rho^2} + \rho \arccos(-\rho)}{2\pi}, \tag{9}$$

while,

$$\mathbb{E}(\mathbf{M}_t^{+}) \;=\; \mathbb{E}(\mathbf{M}_t^{-}) \;=\; (\mathbf{J}_N - \mathbf{I}_N) \times \frac{\rho \arccos \rho - \sqrt{1-\rho^2}}{2\pi}. \tag{10}$$

The off-diagonal elements of the right-hand-side matrices are plotted in Figure 2 as a function of ρ. With perfect negative correlation, the returns are always of opposite sign, and so $\mathcal{P}_t$ and $\mathcal{N}_t$ are both trivially equal zero, while the expectations of $\mathcal{M}_t^{+}$ and $\mathcal{M}_t^{-}$ both equal -0.5. With perfect positive correlation, the two asset returns always have the same sign, which is positive or negative with equal probability, and as a result $\mathcal{P}_t$ and $\mathcal{N}_t$ both equal 0.5 in expectation, while $\mathcal{M}_t^{+}$ and $\mathcal{M}_t^{-}$ are both trivially equal to zero. For $\rho = 0$ the off-diagonal elements of $\mathbb{E}(\mathbf{RCOV}_t) = \mathbb{E}(\mathbf{P}_t + \mathbf{N}_t + \mathbf{M}_t^{+} + \mathbf{M}_t^{-})$ obviously equal zero; the expectations of the off-diagonal elements $\mathcal{P}_t$ and $\mathcal{N}_t$ equal $1/2\pi$, and the expectations of the off-diagonal elements $\mathcal{M}_t^{+}$ and $\mathcal{M}_t^{-}$ equal $-1/2\pi$. As the figure shows, for all other values of ρ the expectations of all the semicovariances differ from zero.

[6]Let r_i denote the daily return on asset i. The off-diagonal elements in $\mathbb{E}(\mathbf{P}_t)$ and $\mathbb{E}(\mathbf{N}_t)$ then equal $\mathbb{E}\left[r_i r_j \mathbf{1}\left\{r_i > 0, r_j > 0\right\}\right]$, while the off-diagonal elements in $\mathbb{E}(\mathbf{M}_t^{+})$ and $\mathbb{E}(\mathbf{M}_t^{-})$ equal $\mathbb{E}\left[r_i r_j \mathbf{1}\left\{r_i > 0, r_j \leq 0\right\}\right]$.

Figure 2: Semicovariances

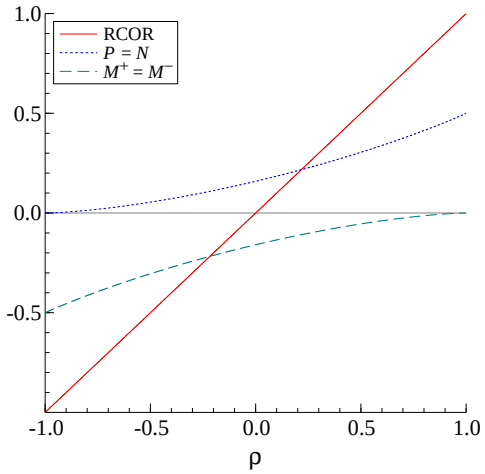

Note: The graph plots the expected semicovariances for a standard normal distribution with correlation ρ, or equivalently the limiting semicovariances under the assumption of a standard Brownian motion with a time-invariant instantaneous correlation ρ and unit variance.

The main idea behind the new realized semicovariance measures, of course, rests on the use of many high-frequency intradaily returns, not the $m = 1$ case considered here. The next section formally establishes that the same right-hand-side expressions for $\mathbb{E}(\mathbf{P}_t)$, $\mathbb{E}(\mathbf{N}_t)$, $\mathbb{E}(\mathbf{M}_t^+)$, and $\mathbb{E}(\mathbf{M}_t^-)$ in (9) and (10) illustrated in Figure 2 obtain as the limiting values of the realized measures for $m \to \infty$ under the assumption that the underlying price process follows a continuous semimartingale with unit volatility and instantaneous correlation ρ. Most importantly, the asymptotic results presented in the next section extend this illustrative setup to allow for more general, and empirically realistic, dynamic dependencies, including stochastic instantaneous volatilities and correlations.

2.2. Asymptotic Theory

Without loss of generality, we will consider the bivariate case, $N = 2$, with quantities defined over the unit time interval. Suppressing the time t subscript, the unique elements in the four 2×2-dimensional realized semicovariance matrices, $\mathbf{P}_t^{(m)}$, $\mathbf{N}_t^{(m)}$, $\mathbf{M}_t^{(m)+}$ and $\mathbf{M}_t^{(m)-}$, may then be gathered in the 8-dimensional random vector process,

$$\mathbf{V}^{(m)} \equiv \begin{bmatrix} \mathcal{V}_1^{(m)+} \\ \mathcal{V}_1^{(m)-} \\ \mathcal{V}_2^{(m)+} \\ \mathcal{V}_2^{(m)-} \\ \mathcal{P}^{(m)} \\ \mathcal{N}^{(m)} \\ \mathcal{M}^{(m)+} \\ \mathcal{M}^{(m)-} \end{bmatrix} = \sum_{k=1}^{m} \begin{bmatrix} r_{k,1}^2 I_{\{r_{k,1}\geq 0\}} \\ r_{k,1}^2 I_{\{r_{k,1}<0\}} \\ r_{k,2}^2 I_{\{r_{k,2}\geq 0\}} \\ r_{k,2}^2 I_{\{r_{k,2}<0\}} \\ r_{k,1} r_{k,2} I_{\{r_{k,1}\geq 0, r_{k,2}\geq 0\}} \\ r_{k,1} r_{k,2} I_{\{r_{k,1}<0, r_{k,2}<0\}} \\ r_{k,1} r_{k,2} I_{\{r_{k,1}\geq 0, r_{k,2}<0\}} \\ r_{k,1} r_{k,2} I_{\{r_{k,1}<0, r_{k,2}\geq 0\}} \end{bmatrix} \equiv \sum_{k=1}^{m} \mathbf{g}(r_{k,1}, r_{k,2}). \quad (11)$$

The first four elements correspond to the positive and negative semivariances of the two assets, while the last four elements refer to the off-diagonal elements in the semicovariance matrices. The following proposition provides the limiting value of $V^{(m)}$ for $m \to \infty$ under the assumption that the underlying price process follows a continuous semimartingale.

Proposition 1 (Semicovariance Limit) *Assume that the bivariate log-price process evolves continuously through time according to the semimartingale,*

$$\mathbf{p}_t = \mathbf{p}_0 + \int_0^t \boldsymbol{\mu}_u du + \int_0^t \boldsymbol{\sigma}_u d\mathbf{W}_u, \qquad 0 \leq t \leq 1, \quad (12)$$

where $\mathbf{W}_u$ denotes a 2-dimensional Brownian motion, $\boldsymbol{\mu}_u$ is a 2-dimensional locally bounded predictable drift process, and $\boldsymbol{\sigma}_u$ is a $\mathbb{R}^{2\times 2}$-valued càdlàg volatility process. Then for $\mathbf{r}_{k,i} \equiv \mathbf{p}_{k/m,i} - \mathbf{p}_{(k-1)/m,i}$, and $m \to \infty$,

$$\mathbf{V}^{(m)} \xrightarrow{p} \int_0^1 \begin{bmatrix} \frac{\sigma_{u,1}^2}{2} \\ \frac{\sigma_{u,1}^2}{2} \\ \frac{\sigma_{u,2}^2}{2} \\ \frac{\sigma_{u,2}^2}{2} \\ \frac{\sigma_{u,1}\sigma_{u,2}}{2\pi}\left(\rho_u \arccos(-\rho_u) + \sqrt{1-\rho_u^2}\right) \\ \frac{\sigma_{u,1}\sigma_{u,2}}{2\pi}\left(\rho_u \arccos(-\rho_u) + \sqrt{1-\rho_u^2}\right) \\ \frac{\sigma_{u,1}\sigma_{u,2}}{2\pi}\left(\rho_u \arccos \rho_u - \sqrt{1-\rho_u^2}\right) \\ \frac{\sigma_{u,1}\sigma_{u,2}}{2\pi}\left(\rho_u \arccos \rho_u - \sqrt{1-\rho_u^2}\right) \end{bmatrix} du \equiv \mathbf{V}, \quad (13)$$

where the convergence holds locally uniform in time, $\sigma_{u,i}^2$ denotes the spot variance of asset i, and ρ_u denotes the spot correlation between the two assets.

The proof of the proposition builds extensively on Barndorff-Nielsen, Graversen,

Jacod, Podolskij, and Shephard (2006) and the extensions thereof in Kinnebrock and Podolskij (2008). Details are provided in the Appendix.

The expectations illustrated in Figure 2 discussed in the previous section correspond to the limiting values that would obtain for $\sigma_{u,1} = \sigma_{u,2} = 1$ and $\rho_u = \rho$, or equivalently a standard time-invariant Brownian motion with unit variance and constant instantaneous correlation ρ. However, as Proposition 1 shows, these same expressions appear in the more general limiting values of the new semicovariance measures.

The proposition above also encompasses the result of Barndorff-Nielsen, Kinnebrock, and Shephard (2010), showing that in the absence of jumps the positive and negative realized semivariance measures each converge in probability to one-half times the integrated variance,

$$\mathcal{V}_i^{(m)+},\ \mathcal{V}_i^{(m)-} \xrightarrow{p} \frac{1}{2}\int_0^1 \sigma_{u,i}^2 du.$$

Correspondingly, large differences between the two realized semivariance measures, $\mathcal{V}_i^{(m)+} - \mathcal{V}_i^{(m)-}$, are naturally interpreted as evidence for discontinuities, or jumps, in the price process for the specific asset i.

Differences in the values of $\mathcal{P}^{(m)}$ and $\mathcal{N}^{(m)}$ may similarly be attributed to the presence of discontinuities occurring at the same time in the two assets, or so-called cojumps, which could affect the measures differently. Of course, differences in the $\mathcal{P}^{(m)}$ and $\mathcal{N}^{(m)}$ realized semicovariance measures may also arise from asymmetries in correlations between positive and negative returns. The following proposition provides a framework for more formally analyzing these differences, under the additional simplifying assumptions of no leverage effects nor volatility jumps. As is standard in the in-fill asymptotic high-frequency data setting, the limiting distribution is random, so that its variance depends on the realization of the underlying process (see, e.g., Mykland and Zhang, 2009).

Proposition 2 (Semicovariance CLT) *Assume that the bivariate log-price process evolves continuously through time according to (12), with the $\boldsymbol{\sigma}_t$ volatility process determined by,*

$$\boldsymbol{\sigma}_t = \boldsymbol{\sigma}_0 + \int_0^t \boldsymbol{\nu}_u' d\mathbf{W}_u^*, \tag{14}$$

where $\boldsymbol{\nu}_u'$ is an adapted càdlàg process, and the 2×2-dimensional Brownian motion $\mathbf{W}_u^*$ is independent of $\mathbf{W}_u$. Then for $m \to \infty$,

$$\sqrt{m}(\mathbf{V}^{(m)} - \mathbf{V}) \xrightarrow{\mathcal{D}_{st}} \int_0^1 \boldsymbol{\alpha}_u d\mathbf{W}_u + \int_0^1 \boldsymbol{\beta}_u d\tilde{\mathbf{W}}_u \equiv \mathbf{U}, \tag{15}$$

where $\xrightarrow{\mathcal{D}_{st}}$ *denotes stable convergence in distribution, the 2-dimensional Brownian motion* $\tilde{\mathbf{W}}_u$ *is independent of* $\mathbf{W}_u$ *and* $\mathbf{W}_u^*$*, and the* 8×2*-dimensional* $\boldsymbol{\alpha}_u$ *and* $\boldsymbol{\beta}_u$ *processes are defined in the Appendix.*

Proof: See Appendix.

Proposition 2 encompasses a number of results in the existing literature as special cases. In particular, utilizing the identity $RCOV^{(m)} = (0,0,0,0,1,1,1,1)\mathbf{V}^{(m)}$, it follows from the definitions of the $\boldsymbol{\alpha}_u$ and $\boldsymbol{\beta}_u$ processes that

$$\sqrt{m}\left[RCOV^{(m)} - \int_0^1 \rho_u \sigma_{u,1}\sigma_{u,2} du\right] \xrightarrow{\mathcal{D}_{st}} MN\left(0, \int_0^1 (1+\rho_u)\sigma_{u,1}^2\sigma_{u,2}^2 dW_u'\right), \quad (16)$$

which corresponds to the well-known result of Barndorff-Nielsen and Shephard (2004a). Considering the linear combination $\mathcal{V}_1^{(m)+} - \mathcal{V}_1^{(m)-} = (1,-1,0,0,0,0,0,0)\mathbf{V}^{(m)}$, the proposition also implies that,

$$\sqrt{m}(\mathcal{V}_1^{(m)+} - \mathcal{V}_1^{(m)-}) \xrightarrow{\mathcal{D}_{st}} MN\left(0, 3\int_0^1 \sigma_{u,1}^4 du\right), \quad (17)$$

consistent with the results of Barndorff-Nielsen, Kinnebrock, and Shephard (2010).

Of course, Proposition 2 further extends the results in the existing literature to allow for the characterization of the asymptotic distributions of other functionals of the new realized semicovariance measures. Specifically, consider the difference between the two conforming semicovariance components $\mathcal{P}^{(m)} - \mathcal{N}^{(m)} = (0,0,0,0,1,-1,0,0)\mathbf{V}^{(m)}$. It follows that

$$\sqrt{m}(\mathcal{P}^{(m)} - \mathcal{N}^{(m)}) \xrightarrow{\mathcal{D}_{st}} MN\left(0, \int_0^1 \frac{\sigma_{u,1}^2\sigma_{u,2}^2}{\pi}\left((1+2\rho_u^2)\arccos(-\rho_u) + 3\rho_u\sqrt{1-\rho_u^2}\right) du\right). \quad (18)$$

Similarly, for the realized semicovariance components of opposite signs, their difference $\mathcal{M}^{(m)+} - \mathcal{M}^{(m)-} = (0,0,0,0,0,0,1,-1)\mathbf{V}^{(m)}$ is asymptotically distributed as,

$$\sqrt{m}(\mathcal{M}^{(m)+} - \mathcal{M}^{(m)-}) \xrightarrow{\mathcal{D}_{st}} MN\left(0, \int_0^1 \frac{\sigma_{u,1}^2\sigma_{u,2}^2}{\pi}\left((1+2\rho_u^2)\arccos(-\rho_u) - 3\rho_u\sqrt{1-\rho_u^2}\right) du\right). \quad (19)$$

The mutually exclusive indicator functions underlying the definitions of the different semicovariance components, further implies that $\mathcal{P}^{(m)} - \mathcal{N}^{(m)}$ and $\mathcal{M}^{(m)+} - \mathcal{M}^{(m)-}$ are asymptotically independent. Correspondingly, the distributions of these quantities may be used in the formulation of asymptotically independent tests for equality of the respective semicovariance components.

Of course, the actual empirical implementation of the mixed-normal distributions in (18) and (19) also necessitates a way to quantify the asymptotic variances. More generally, the implementation of any distributional results based on Proposition 2 and the result in (15), requires a way to estimate the elements in the asymptotic covariance matrix,

$$\mathbf{\Pi} \equiv Var(\mathbf{U}) = \int_0^1 (\boldsymbol{\alpha}_u \boldsymbol{\alpha}_u' + \boldsymbol{\beta}_u \boldsymbol{\beta}_u') du. \tag{20}$$

The following proposition provides a general framework for doing so.

Proposition 3 (Feasible CLT) *Under the same assumptions as for Proposition 2, and for* $m \to \infty$*,*

$$\mathbf{\Pi}^{(m)} \xrightarrow{p} \mathbf{\Pi}, \tag{21}$$

and

$$\{\mathbf{\Pi}^{(m)}\}^{-1/2} \sqrt{m}(\mathbf{V}^{(m)} - \mathbf{V}) \xrightarrow{\mathcal{D}} N(0, \mathbf{I}), \tag{22}$$

where the $(a,b)^{th}$ *element in the* $\mathbf{\Pi}^{(m)}$ *matrix is given by,*

$$\Pi_{a,b}^{(m)} \equiv m \sum_{k=1}^{m} g_a(r_{k,1}, r_{k,2}) g_b(r_{k,1}, r_{k,2}) - \sum_{k=1}^{m} g_a(r_{k,1}, r_{k,2}) \sum_{k=1}^{m} g_b(r_{k,1}, r_{k,2}), \tag{23}$$

and g_a *refers to the* a^{th} *element in the vector-function* $\mathbf{g}$ *defined in (11).*

Proof: See Appendix.

To illustrate, consider the test for $\mathcal{P} = \mathcal{N}$ based on the mixed-normal distribution in (18). Proposition 3 implies that $\sqrt{m}(\mathcal{P}^{(m)} - \mathcal{N}^{(m)})$ divided by,

$$\pi^{(m)} \equiv m \sum_{k=1}^{m} \left[r_{k,1}^2 r_{k,2}^2 I_{\{r_{k,1} \geq 0, r_{k,2} \geq 0\}} + r_{k,1}^2 r_{k,2}^2 I_{\{r_{k,1} < 0, r_{k,2} < 0\}} \right] - (\mathcal{P}^{(m)} - \mathcal{N}^{(m)})^2, \tag{24}$$

is asymptotically standard normally distributed. As such, this allows for the construction of an easy-to-calculate test statistic for testing the hypothesis that $\mathcal{P} = \mathcal{N}$.[7] A similar approach and feasible expression may be obtained for testing the equality of $\mathcal{M}^+$ and $\mathcal{M}^-$.

The consistency of the simple variance estimator $\pi^{(m)}$ defined above relies on the semimartingale assumption and would otherwise diverge in the presence

[7] General nonparametric procedures, like the two-scales observed asymptotic variance recently developed by Mykland and Zhang (2017), or a bootstrap type approach, as in Goncalves and Meddahi (2009), might alternatively be used for calculating asymptotically valid standard errors.

of cojumps. Correspondingly, the test statistic obtained using this estimator to normalize $\sqrt{m}(\mathcal{P}^{(m)} - \mathcal{N}^{(m)})$ will only be consistent for detecting differences in $\mathcal{P}$ and $\mathcal{N}$ stemming from continuous prices moves and asymmetries in correlations.

To obtain power against cojumps, one can follow Mancini (2009) and truncate the high-frequency returns used in the calculation of the asymptotic variance, and the construction of second version of the test using this jump-robust estimator, denoted $\pi_{Tr}^{(m)}$, to normalize the difference.[8] In the simulation and empirical results discussed below, we rely on the same dynamic threshold advocated by Bollerslev and Todorov (2011a,b) based on three times the trailing scaled bipower variation, further adjusted for the strong intraday periodicity in the volatility.[9]

We turn next to a discussion of a small scale Monte Carlo simulation study designed to investigate the accuracy of these feasible approximations to the asymptotic distributional results in Propositions 1-3, and the power of the two different versions of the test for $\mathcal{P} = \mathcal{N}$ to detect cojumps and/or asymmetries in correlations, in particular.

2.3. Finite Sample Simulations

We begin by considering the simulations from a simple bivariate price process $d\mathbf{p}_u = \boldsymbol{\sigma}_u d\mathbf{W}_u$, with constant diffusive volatility matrix $\boldsymbol{\sigma}_u\boldsymbol{\sigma}_u' \equiv (1-\rho)\mathbf{I}_2 + \rho\mathbf{J}_2$, where $\mathbf{I}_2$ is the 2×2 identity matrix and $\mathbf{J}_2$ is a 2×2 matrix of ones. This parallels the illustrative example discussed in Section 2.1, with the limiting values for the different semicovariances depicted in Figure 2. This simple simulation setup obviously adheres to the assumptions underlying Propositions 1-3, and as such speaks to the size of the tests based on these propositions. Following the discussion in the previous section, we consider two versions of the test: one using the "raw" asymptotic variance estimator to normalize the $\mathcal{P} - \mathcal{N}$ difference, and another using the jump-robust truncated variance estimator. The data are generated using a standard Euler discretization scheme based on 23,400 observations per "day," corresponding to one-second sampling in a 6.5 hour market, like the U.S. equity market data analyzed below.

The top panel in Table 1 reports the rejection frequencies averaged across 10,000 replications for different significance levels (10%, 5%, and 1%), sampling

[8] This mirrors the arguments of Barndorff-Nielsen and Shephard (2004b, 2006) and the need to normalize the difference between the realized variance and the bipower variation by a jump-robust variance estimator to ensure power against individual asset specific jumps.

[9] Thus $\pi_{Tr}^{(m)}$ is based on equation (24) but using truncated returns $\tilde{r}_{t,k,i} = r_{t,k,i}\mathbf{1}\left\{|r_{t,k,i}| \leq \alpha_{t,k,i}\Delta^{0.49}\right\}$, where $\alpha_{t,k,i} = 3\sqrt{BPV_{t-1,i}} \times TOD_{k,i}$; see Bollerslev and Todorov (2011b) for details.

frequencies m (78 and 26, corresponding to 5 and 15-minute returns, respectively), and correlations ρ (0.0 and 0.5).[10] As is evident, the simple version of the test based on $\pi^{(m)}$ is generally well sized. Meanwhile, since the truncation invariably reduces the magnitude of the normalizing variance, there is a tendency for the test that relies on the jump-robust $\pi_{Tr}^{(m)}$ estimator to over-reject, especially for coarser sampling frequencies and higher correlations, albeit not dramatically so.

To investigate the power of the tests, the middle panel of Table 1 shows the rejection frequencies from a simulation with cojumps.[11] In particular, following the simulation setup of Caporin, Kolokolov, and Renò (2017), we add randomly distributed jumps of size $N(8/\sqrt{78}, 2/\sqrt{78})$ to each of the two series at a single random point each "day." As expected, the test based on $\pi^{(m)}$ deteriorates and almost never rejects in this situation. On the other hand, the use of $\pi_{Tr}^{(m)}$ for the normalization leads to a very powerful test, with rejection frequencies close to unity at all of the three different nominal levels.

Differences in the concordant semicovariance elements and violations of the asymptotic distributional results may, of course, also arise from dynamic leverage effects and asymmetries in correlations.[12] The final panel of the table reports on the power of the tests to detect these types of deviations from the null. Specifically, depending on whether the simulated $dW_{s,1}$ price increment for the first asset is positive/negative, we decrease/increase the instantaneous correlation ρ by 0.05.[13] In contrast to the previous cojump alternative, the two different versions of the test both exhibit good power in this situation. This suggest that by comparing the outcome of the $\pi^{(m)}$ and $\pi_{Tr}^{(m)}$ based tests it may be possible to differentiate between alternate influences and types of economic events that cause $\mathcal{P}$ and $\mathcal{N}$ to differ. We will briefly return to this in our discussion of the actual empirical application of these tests below.

[10] Results for other sampling frequencies and correlations are available in the Supplemental Appendix, as are the results for testing $\mathcal{M}^+ = \mathcal{M}^-$. We also considered a setup with $\boldsymbol{\sigma}_u \boldsymbol{\sigma}_u' \equiv \varsigma_u[(1-\rho)\mathbf{I}_2 + \rho \mathbf{J}_2]$, with the same ς_u diurnal pattern as in Andersen, Dobrev, and Schaumburg (2012). The results from these additional simulations are almost identical to the ones reported here; further details are again available in the Supplementary Appendix.

[11] There is ample empirical evidence that most asset prices occasionally jump, and that jumps often occur at the same time for multiple assets; see, e.g., Bollerslev, Law, and Tauchen (2008), Jacod and Todorov (2009), Lahaye, Laurent, and Neely (2011), and Aït-Sahalia and Xiu (2016).

[12] As noted above, there is ample empirical evidence of asymmetries in return correlations; see, e.g., Longin and Solnik (2001), Ang and Chen (2002), and Poon, Rockinger, and Tawn (2004).

[13] This asymmetric correlation process is related to the "Tanaka equation," and it violates the càdlàg assumption of Proposition 1, as the process is not Lipschitz continuous. Alternatively, it may interpreted as an approximation to an infinite activity jump volatility process. However, given the set-up the limits of $\mathcal{P}$ and $\mathcal{M}^+$ clearly converge to their standard limits with $\rho^+ = \rho + 0.05$, while $\mathcal{N}$ and $\mathcal{M}^-$ converge to limits with $\rho^- = \rho - 0.05$.

Table 1: Simulation Results

m	ρ	$\pi^{(m)}$			$\pi^{(m)}_{Tr}$		
		10%	5%	1%	10%	5%	1%
				$\mathcal{H}_0$			
78	0	0.108	0.053	0.009	0.130	0.070	0.018
78	0.5	0.099	0.048	0.009	0.153	0.092	0.028
26	0	0.116	0.052	0.006	0.144	0.083	0.027
26	0.5	0.116	0.056	0.010	0.180	0.113	0.046
				$\mathcal{H}_A$: Cojumps			
78	0	0.001	0.001	0.000	0.992	0.990	0.984
78	0.5	0.006	0.001	0.000	0.973	0.962	0.928
26	0	0.010	0.003	0.000	0.936	0.920	0.885
26	0.5	0.028	0.008	0.001	0.848	0.807	0.722
				$\mathcal{H}_A$: Asymmetric Correlations			
78	0	0.960	0.920	0.755	0.960	0.925	0.782
78	0.5	0.915	0.855	0.644	0.934	0.887	0.725
26	0	0.944	0.870	0.553	0.944	0.877	0.584
26	0.5	0.898	0.804	0.493	0.914	0.838	0.557

Note: The table reports the rejection frequencies for testing the "daily" $\mathcal{P} = \mathcal{N}$ based on 10,000 replications. The $\pi^{(m)}$ and $\pi^{(m)}_{Tr}$ versions of the tests rely on the standard and truncated variance for normalizing the difference. The data are generated from a continuous price process $d\mathbf{P}_u = \boldsymbol{\sigma}_u d\mathbf{W}_u$ aggregated to the five and fifteen "minute" frequency, corresponding to $m = 78$ and $m = 26$ observation per "day." The null hypothesis ($\mathcal{H}_0$) postulates a constant spot covariance matrix, $\boldsymbol{\sigma}_u\boldsymbol{\sigma}'_u \equiv [(1-\rho)\mathbf{I}_2 + \rho\mathbf{J}_2]$ for all u. The first alternative hypothesis ($\mathcal{H}_A$) adds cojumps of random size $N(8/\sqrt{78}, 2/\sqrt{78})$ at a single random time each "day." The second alternative hypothesis ($\mathcal{H}_A$) has dynamically varying spot correlations, determined by $[(1-(\rho+0.05))\mathbf{I}_2 + (\rho+0.05)\mathbf{J}_2]$ if $W_{s,1} < 0$, and $[(1-(\rho-0.05))\mathbf{I}_2 + (\rho-0.05)\mathbf{J}_2]$ if $W_{s,1} > 0$.

Overall, the simulation results clearly corroborate the accuracy of the asymptotic results for making valid finite-sample inference, and the practical usefulness of the tests for detecting significant differences in the concordant semicovariance elements, whether due to cojumps and/or asymmetric dynamically varying correlations.[14]

[14]The two versions of the test analyzed here afford a distinction between cojumps and asym-

3. Empirical Analysis of Realized Semicovariances

This section highlights some of the key distributional features and information conveyed by the new realized semicovariance measures. Before doing so, however, we briefly discuss the data and practical implementation underlying our empirical investigations.

3.1. Data

Our analysis relies on high-frequency intradaily equity prices obtained from the Trades and Quotes (TAQ) database. We restrict our sample to the S&P 500 constituent stocks with at least 2,000 daily observations during our January 1993 to December 2014 sample period, for a total of 749 unique stocks. The asymptotic results pertaining to the new realized semicovariance measures discussed in the previous section formally rely on $m \to \infty$, or the notion of ever finer sampled high-frequency returns. In practice, a host of market microstructure complications prevent us from sampling too frequently, while maintaining the fundamental no-arbitrage semimartingale assumption (see, e.g., the discussion in Hansen and Lunde (2006), and Jacod, Li, and Zheng (2017)). In the multivariate context these complications are compounded by non-synchronous prices and the so-called Epps (1979) effect. In an effort to strike a reasonable balance between these conflicting goals of sampling as frequently as possible on the one hand, and maintaining the martingale assumption as a sensible approximation on the other, we rely on a 15-minute sampling frequency, or $m = 26$ observations per trade day; a similar choice, and a more detailed justification thereof, was adopted by Bollerslev, Law, and Tauchen (2008).[15] Like much past work in volatility forecasting (e.g., Aït-Sahalia and Xiu (2017), Hansen, Huang, and Shek (2012), and Noureldin, Shephard, and Sheppard (2012)) we focus only on the intra-daily period in our analyses, and exclude overnight returns.[16]

metric correlations without jumps. To further differentiate between asymmetric correlations with or without cojumps, a second truncated version of the test in which the realized semicovariance measures themselves are constructed from truncated high-frequency returns could be used. Additional simulation results for this third version of the test are available in the Supplemental Appendix.

[15]This particular choice of m, of course, also mirrors the sampling frequency analyzed in the simulations discussed in the previous section.

[16]The Supplemental Appendix contains additional empirical results including the overnight returns. All of the key findings discussed below remain intact, and if anything some of the forecasting results are even stronger.

Figure 3: Tests for Semicovariance Equality

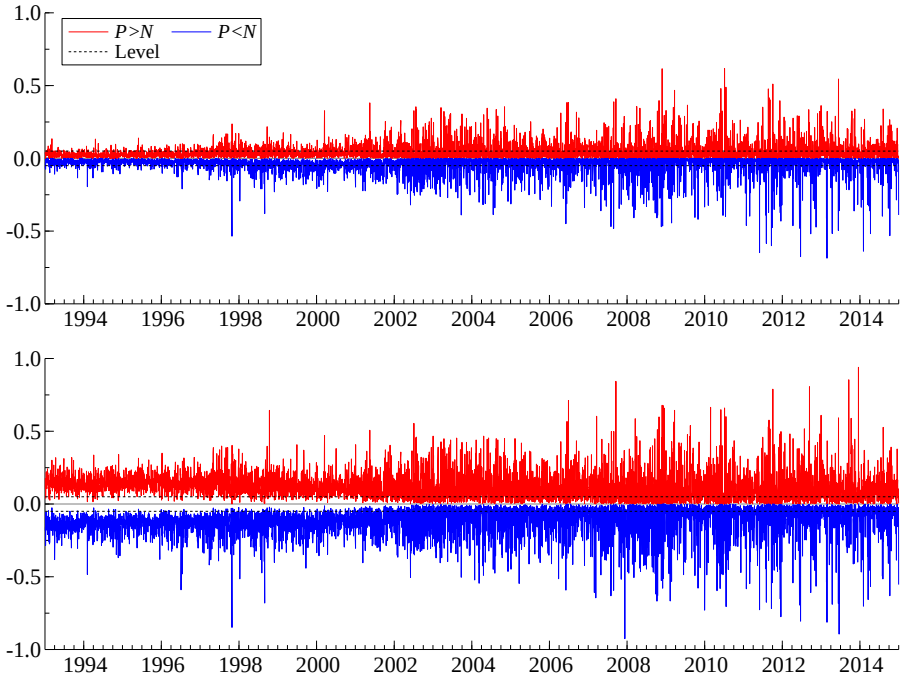

Note: The figure shows the rejection frequencies for testing the hypotheses that $\mathcal{P} > \mathcal{N}$ and $\mathcal{P} < \mathcal{N}$ at the 5% level for 1,000 randomly selected pairs of stocks for each of the days in the 1993-2014 sample. The top panel is based on the non-jump robust variance estimator $\pi^{(m)}$, while the bottom panel uses the truncated variance estimator $\pi_{Tr}^{(m)}$ to normalize the difference.

3.2. Tests for the Equality of Semicovariances

We begin by testing equality of positive and negative semicovariances ($\mathcal{P}$ and $\mathcal{N}$) using the two different versions of the test analyzed in the simulations in Section 2.3. Specifically, selecting 1,000 random pairs of stocks, Figure 3 graphs the resulting rejection frequencies for testing $\mathcal{P} > \mathcal{N}$ and $\mathcal{P} < \mathcal{N}$ at the 5% level for each of the 5,541 days in the sample. The top panel gives the results for the version of the test based on the simple $\pi^{(m)}$ estimator, while the tests in the bottom panel rely on the truncated $\pi_{Tr}^{(m)}$ estimator to normalize the difference.

Looking at the top panel, the unconditional rejection frequencies appear fairly close to the nominal size of the test. However, the rejections that do occur clearly cluster in time, and tend to increase during periods of high volatility and market turmoil. Also, even though the rejection frequencies for $\mathcal{P} < \mathcal{N}$ appear slightly large than those for $\mathcal{P} > \mathcal{N}$ on a few select days, especially over the last few years of the sample, the two rejection frequencies are almost the same when averaged over the full sample.

Turning to the bottom panel and the tests based on $\pi_{Tr}^{(m)}$, the figure obviously indicate many more rejections on average, with roughly the same number of rejections in either direction. The rejection frequencies also appear more evenly distributed through time, than do the tests based on $\pi^{(m)}$ in the top panel. The on average higher number of rejections is, of course, to be expected as the truncated version of the test not only exhibits power against asymmetric correlations but also cojumps. The finding that the rejection frequencies for the $\pi_{Tr}^{(m)}$-based tests appear much more evenly distributed over the full sample is also in line with Aït-Sahalia and Xiu (2016), who report that the relative contribution to the realized covariation stemming from cojumps versus diffusive price moves seems fairly stable through time.

To help understand what drive these differences, Table 2 reports the five days on which the two different versions of the test reject the most. In addition to the date and the rejection frequencies, we also note the most important economic events that occurred on each of the days.Interestingly, the days with the most rejections for the test based on $\pi^{(m)}$ are typically associated with "soft," or diffusive and difficult to interpret information, like the outcome of the Italian Election or the start of Janet Yellen's tenure as chair of the Federal Reserve Board. By contrast, all but one of the top rejection days for the $\pi_{Tr}^{(m)}$-based test are readily associated with macroeconomic news announcements in the form of FOMC statements or rate decisions. Putting these results further into perspective, individual jump tests, corresponding to significant differences between positive and negative semivariances ($\mathcal{V}^+$ and $\mathcal{V}^-$), have previously been associated with either macroeconomic news announcements or firm specific news events (e.g., Lee and Mykland (2008) and Lee (2012)), while tests for cojumps, or significant differences between semicovariances ($\mathcal{P}$ and $\mathcal{N}$), are naturally associated with only economy wide news that affect all assets (e.g., Bollerslev, Law, and Tauchen (2008) and Lahaye, Laurent, and Neely (2011)). We will not pursue this event type analysis any further here, turning instead to a discussion of the general dynamic dependencies inherent in each of the different realized semicovariance measures.[17]

3.3. Dynamic Dependencies

The previously discussed Figure 1 showing the time series of realized semicovariances clearly suggests very different dynamic dependencies in the concordant

[17]The Supplemental Appendix contains a table with additional rejection days to extend Table 2, as well as the results for the double-truncated version of the tests discussed in Footnote 14 above. Also presented are results comparing the rejection frequencies with those of other univariate jump tests and volatility measurement procedures.

Table 2: Top Rejection Days

Date	Direction	%	Event
$\pi^{(m)}$			
25-02-2013	$\mathcal{N} > \mathcal{P}$	69	Italian elections
21-06-2012	$\mathcal{N} > \mathcal{P}$	68	Rumors of Moody downgrade for global banks
01-06-2011	$\mathcal{N} > \mathcal{P}$	65	Moody's cut Greece's bond rating by three notches
03-02-2014	$\mathcal{N} > \mathcal{P}$	64	Janet Yellen sworn in as new Fed chair
26-11-2008	$\mathcal{P} > \mathcal{N}$	62	Bank of America acquisition of Merill Lynch approval
$\pi_{Tr}^{(m)}$			
18-12-2013	$\mathcal{P} > \mathcal{N}$	94	Fed reduction of Asset Buying Program
11-12-2007	$\mathcal{N} > \mathcal{P}$	93	Fed drops rate by 25 basis points
19-06-2013	$\mathcal{N} > \mathcal{P}$	89	Announcement that Fed will continue buying Mortgage Backed Securities
27-10-1997	$\mathcal{P} > \mathcal{N}$	85	Mini-crash and NYSE circuit breaker trading halt
18-09-2013	$\mathcal{P} > \mathcal{N}$	85	Announcement that Fed will sustain Asset Buying Program

Note: The table reports the five days of most one-sided rejections for the test of $\mathcal{P}_{ij} = \mathcal{N}_{ij}$. The first column gives the date, the second provides the direction in which the rejections occurred, and the third column provides the fraction of pairs where equality is rejected in that direction. The final column provides a description of the event. The top panel is based on a non-jump robust variance estimator $\Pi^{(m)}$, while the bottom panel uses the truncated variance estimator $\Pi_{Tr}^{(m)}$ to normalize the difference.

($\mathcal{P}_t$ and $\mathcal{N}_t$) and discordant ($\mathcal{M}_t$) elements. In Figure 4 we present autocorrelations, computed using the estimator of Hansen and Lunde (2014) to account for measurement errors, averaged across 1,000 randomly selected pairs of stocks. Whereas the autocorrelations for the realized variances (RV_t) and the positive and negative realized semivariances ($\mathcal{V}_t^+$ and $\mathcal{V}_t^-$) shown in the left panel are almost indistinguishable,[18] there is a clear ordering in the rate of decay of the autocorrelations for the realized semicovariance elements shown in the right panel. Most noticeably, the autocorrelations for $RCOV_t$ are systematically below those for the three realized semicovariance elements, with the mixed $\mathcal{M}_t$ term exhibiting the highest overall persistence, and $\mathcal{P}_t$ and $\mathcal{N}_t$ decaying very similarly.[19]

[18]This contrasts with Patton and Sheppard (2015), who found the negative realized semivariances to be more persistent than the realized variances. However the results presented here differ in that they are based on a wider sample of stocks and use the autocorrelation estimator

Figure 4: Autocorrelations

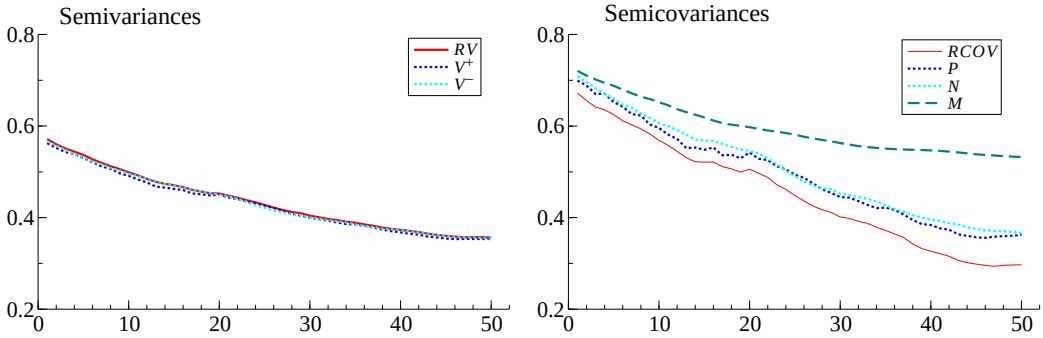

Note: The graph plots the autocorrelation functions for the different realized semicovariance elements. All of the estimates are averaged across 1,000 randomly selected pairs of stocks, and bias adjusted following the approach of Hansen and Lunde (2014).

These marked differences in the serial dependencies imply that different univariate time series models would be required for satisfactorily modeling each of the different realized semicovariance elements. Importantly, they also suggest that more accurate volatility and covariance matrix forecasts may be obtained by "looking inside" the covariance matrix and separately modeling and forecasting the $\mathcal{P}_t$, $\mathcal{N}_t$, and $\mathcal{M}_t$ components that make up $RCOV_t$.

In order to more explicitly investigate this conjecture and further characterize the dynamic dependencies inherent in the semicovariances, we estimate a vector version of the popular HAR model of Corsi (2009), in which each of the elements in the realized semicovariance matrix are allowed to depend on its own "daily," "weekly," and "monthly" lags, as well as the lags of the other realized semicovariance components. That is,

$$\begin{bmatrix} \mathcal{P}_{ij,t} \\ \mathcal{N}_{ij,t} \\ \mathcal{M}_{ij,t} \end{bmatrix} = \begin{bmatrix} \phi_{\mathcal{P}ij} \\ \phi_{\mathcal{N}ij} \\ \phi_{\mathcal{M}ij} \end{bmatrix} + \mathbf{\Phi}_{ij,D} \begin{bmatrix} \mathcal{P}_{ij,t-1} \\ \mathcal{N}_{ij,t-1} \\ \mathcal{M}_{ij,t-1} \end{bmatrix} + \mathbf{\Phi}_{ij,W} \begin{bmatrix} \mathcal{P}_{ij,t-2:t-5} \\ \mathcal{N}_{ij,t-2:t-5} \\ \mathcal{M}_{ij,t-2:t-5} \end{bmatrix} + \mathbf{\Phi}_{ij,M} \begin{bmatrix} \mathcal{P}_{ij,t-6:t-22} \\ \mathcal{N}_{ij,t-6:t-22} \\ \mathcal{M}_{ij,t-6:t-22} \end{bmatrix} + \begin{bmatrix} \epsilon_t^{\mathcal{P}ij} \\ \epsilon_t^{\mathcal{N}ij} \\ \epsilon_t^{\mathcal{M}ij} \end{bmatrix}, \tag{25}$$

of Hansen and Lunde (2014).

[19] In the presence of jumps, and in particular *co-jumps*, $\mathcal{P}_t$, $\mathcal{N}_t$ and $\mathcal{M}_t$ will all depend on the continuous variation in returns, while only $\mathcal{P}_t$ and $\mathcal{N}_t$ will be affected by (co-)jumps. Jump variation is generally thought to be less persistent than continuous variation (see, e.g., the theoretical pricing models in Duffie, Pan, and Singleton (2000) and the empirical evidence in Andersen, Bollerslev, and Diebold (2007) and Corsi, Pirino, and Renò (2010)), and as such one may naturally expect $\mathcal{M}_t$ to be the more persistent component.

Table 3: Semicovariance HAR Estimates

	$\mathcal{P}_{ij,t}$	$\mathcal{N}_{ij,t}$	$\mathcal{M}_{ij,t}$	$RCOV_{ij,t}$
$\mathcal{P}_{ij,t-1}$	0.038*	0.050*	-0.035*	0.052**
$\mathcal{P}_{ij,t-2:t-5}$	0.004	0.057	-0.002	0.059
$\mathcal{P}_{ij,t-6:t-22}$	-0.074	0.023	0.099	0.048
$\mathcal{N}_{ij,t-1}$	0.248**	0.192**	-0.096**	0.344**
$\mathcal{N}_{ij,t-2:t-5}$	0.312**	0.250**	-0.090*	0.472**
$\mathcal{N}_{ij,t-6:t-22}$	0.349**	0.206*	-0.021	0.534**
$\mathcal{M}_{ij,t-1}$	-0.075*	-0.072*	0.141**	-0.006
$\mathcal{M}_{ij,t-2:t-5}$	-0.044	-0.049	0.209**	0.116
$\mathcal{M}_{ij,t-6:t-22}$	0.028	-0.020	0.409**	0.417**

Note: The table reports the average parameter estimates for the vector HAR model in (25) averaged across 500 randomly selected pairs of stocks. The first three columns reports results for the unrestricted models. The last column reports the estimates that restricts the rows of Φ_D, Φ_W and Φ_M to be the same, corresponding to a model for $RCOV_{ij,t}$. ** and * signify that the estimates for that coefficient are significant at the 5% level for 75% and 50% of the randomly selected pairs of stocks, respectively.

where $\mathcal{P}_{ij,t-l:t-k} \equiv \frac{1}{k-l+1}\sum_{s=l}^{k}\mathcal{P}_{ij,t-s}$, with the other terms defined analogously.[20]

The first three columns of Table 3 report the OLS-based parameter estimates averaged across 500 randomly selected pairs of stocks. To aid interpretation, we also include stars to signify the proportion of the coefficient estimates across the 500 random pairs of stocks that are significant at the usual 5% level. The table reveals a clear block structure in the coefficients for the general specification reported in the first three columns. Most notably, the dynamic dependencies in $\mathcal{P}_t$ and $\mathcal{N}_t$ are almost exclusively driven by the lagged $\mathcal{N}_t$ terms. By contrast, the dynamics of the mixed $\mathcal{M}_t$ elements are primarily determined by their own lags, with the monthly lag receiving by far the largest weight.

The last column of Table 3 reports the parameter estimates from regressing $RCOV_t$ on the lagged realized semicovariances, or equivalently a HAR model as in (25) in which the rows of $\mathbf{\Phi}_D$, $\mathbf{\Phi}_W$ and $\mathbf{\Phi}_M$ are restricted to be the same. As is evident, the same block structure remains, with the three lags of $\mathcal{N}_t$ and the monthly lag of $\mathcal{M}_t$ constituting the main drivers of $RCOV_t$. Putting the estimates further into perspective, on average $\mathcal{P}_t/RCOV_t = 0.837, \mathcal{N}_t/RCOV_t = 0.847$ and $\mathcal{M}_t/RCOV_t = -0.684$, so that normalizing each of the explanatory variables,

[20]Note that the "weekly" variable excludes the daily lag, and the "monthly" variable excludes the daily and weekly lags. This aids interpretation but does not affect the fit of the model.

the semicovariance-based HAR models effectively put a weight of approximately 0.339 on lagged daily information. By comparison, the average estimates for a standard HAR model for $RCOV_t$ equal 0.184, 0.305 and 0.304 for the daily, weekly and monthly lag, respectively, leading to a more muted reaction to new daily information.

The distinct dynamic dependencies revealed in the realized semicovariance components suggest that covariance matrix forecasting models may be improved by using these components separately, rather than relying solely on realized covariance measures. Empirical results reported in the Supplemental Appendix thoroughly corroborate this in applications to covariance matrix forecasts ranging from bivariate to 100-dimensional. Going one step further, we next demonstrate how realized semicovariance measures may also be used in the construction of improved univariate portfolio volatility forecasts by "looking inside" the covariance matrix of the assets that make up the portfolio.

3.4. Semicovariances and Portfolio Volatility Forecasting

As discussed in Barndorff-Nielsen, Kinnebrock, and Shephard (2010) and Patton and Sheppard (2015), the realized variance of a portfolio may be decomposed into the positive and negative realized semivariances based on high-frequency portfolio returns. Given high-frequency returns for all of the constituent assets of the portfolio, the portfolio realized variance can also be decomposed into three separate semicovariance components. In particular, utilizing the identity $RCOV_t = \mathcal{P}_t + \mathcal{N}_t + \mathcal{M}_t$, it follows readily that for any vector of portfolio weights, say $\mathbf{w}$,

$$\begin{aligned} RV_t^p &\equiv \mathbf{w}'\mathbf{RCOV}_t\mathbf{w} \\ &= \mathbf{w}'\mathbf{P}_t\mathbf{w} \;+\; \mathbf{w}'\mathbf{N}_t\mathbf{w} \;+\; \mathbf{w}'\mathbf{M}_t\mathbf{w} \\ &\equiv \mathcal{P}_t^p \;+\; \mathcal{N}_t^p \;+\; \mathcal{M}_t^p, \end{aligned} \tag{26}$$

where the p superscript indicates the relevant univariate portfolio quantities. Note that the $\mathcal{P}_t^p$ and $\mathcal{N}_t^p$ portfolio semicovariance measures are distinctly different from the corresponding univariate portfolio semivariances, as the latter depend only on the aggregate portfolio return and its sign, whereas the former use returns on *all* of the constituents stocks in the portfolio. The results in the previous section suggest that lagged values of the $\mathcal{P}_t^p$, $\mathcal{N}_t^p$ and $\mathcal{M}_t^p$ realized portfolio semicovariance measures may convey different information about future realized portfolio variances. We next explore this empirically by comparing the forecasts form a series of competing forecasting models.

3.4.1. Forecast Comparisons

The simple and easy-to-implement HAR model of Corsi (2009) has arguably emerged as the benchmark model for judging alternative realized volatility-based forecasting procedures. One-day-ahead forecasts for the portfolio return variance from the model are constructed as,

$$RV^p_{t+1|t} \;=\; \phi_0 \;+\; \phi_d RV^p_t \;+\; \phi_w RV^p_{t-1:t-4} \;+\; \phi_m RV^p_{t-5:t-21}. \tag{27}$$

In addition to this commonly used benchmark, we also consider the forecasts from the Semivariance HAR (SHAR) model of Patton and Sheppard (2015), in which the daily realized variance is decomposed into its realized semivariance components,

$$RV^p_{t+1|t} \;=\; \phi_0 \;+\; \phi_{d,+}\mathcal{V}^{+p}_t \;+\; \phi_{d,-}\mathcal{V}^{-p}_t \;+\; \phi_w RV^p_{t-1:t-4} \;+\; \phi_m RV^p_{t-5:t-21}. \tag{28}$$

This model has been found to perform particularly well from the perspective of portfolio variance forecasting, performing on par with or better than the forecasts from other HAR-style models.[21]

To investigate the benefit of decomposing not only the realized variance, but also the realized covariance, we extend the SHAR model to allow the forecasts to depend on each of the realized portfolio semicovariance components,

$$\begin{aligned} RV^p_{t+1|t} \;=\; \phi_0 \;+\; \phi_{d,\mathcal{P}}\mathcal{P}^p_t \;+\; \phi_{w,\mathcal{P}}\mathcal{P}^p_{t-1:t-4} + \; \phi_{m,\mathcal{P}}\mathcal{P}^p_{t-5:t-21} \\ +\; \phi_{d,\mathcal{N}}\mathcal{N}^p_t \;+\; \phi_{w,\mathcal{N}}\mathcal{N}^p_{t-1:t-4} + \; \phi_{m,\mathcal{N}}\mathcal{N}^p_{t-5:t-21} \\ +\; \phi_{d,\mathcal{M}}\mathcal{M}^p_t \;+\; \phi_{w,\mathcal{M}}\mathcal{M}^p_{t-1:t-4} + \; \phi_{m,\mathcal{M}}\mathcal{M}^p_{t-5:t-21}. \end{aligned} \tag{29}$$

We will refer to the corresponding model as the SemiCovariance HAR (SCHAR) model. The SCHAR model is obviously quite richly parameterized. Hence, motivated by the distinct dynamic dependencies in the different realized semicovariance components documented in the previous section, we also consider a restricted version, in which we only include the daily, weekly and monthly lags of $\mathcal{N}^p$, together with the monthly lag of $\mathcal{M}^p$; i.e, we fix $\phi_{d,\mathcal{P}} = \phi_{w,\mathcal{P}} = \phi_{m,\mathcal{P}} = \phi_{d,\mathcal{M}} = \phi_{w,\mathcal{M}} = 0$. We will refer to the forecasts from this restricted specification as SCHAR-r for short.

[21] Bollerslev, Patton, and Quaedvlieg (2016) provide a recent detailed empirical forecast comparison of the SHAR model with a list of other univariate HAR models, including the HARQ model and models that explicitly allow for jumps.

We consider portfolios comprised of between $N = 1$ and $N = 100$ individual stocks. For each portfolio dimension N, we randomly select 500 stocks, restricting the selected stocks to contain an overlap of at least 1,100 daily observations. We then construct rolling out-of-sample forecasts based on each of the different models, in which all of the model parameters are re-estimated (by least-squares) daily using the most recent 1,000 daily observations. We rely on the commonly-used MSE and QLIKE loss functions to evaluate the performance of the resulting $RV^p_{t+1|t}$ forecasts vis-a-vis the actual realized portfolio volatilities RV^p_{t+1}.[22]

Table 4 reports the results for $N = 1, 10$ and 100. The first column in each panel reports the loss averaged across time and stocks. For each of the 500 samples, we also compute the ratio of each model's average loss relative to the standard HAR model. The second column in each panel reports the average of these ratios over all of the random samples.[23]

For the univariate case, $N = 1$, we find results that are consistent with those of Patton and Sheppard (2015): the SHAR-based forecasts outperform the standard HAR-based forecasts, albeit not by much in our sample.[24] Meanwhile, for larger values of N and portfolios comprised of more than one stock, utilizing the information in the realized semicovariances can result in quite substantial improvements in the accuracy of the forecasts compared to the HAR and SHAR-based forecasts that only rely on the realized portfolio (semi)variances. The results for the QLIKE loss function, in particular, also clearly highlight the advantages of the SCHAR-r specification compared to the forecasts from the unrestricted SCHAR model that entail a large number of freely estimated parameters. The fact that the restricted SCHAR-r model performs the best from a forecasting perspective is, of course, entirely consistent with the extensive evidence in the forecasting literature emphasizing the importance of parsimony (see, e.g., Zellner (1992)).

To further visualize these findings, Figure 5 plots the median loss ratios for the HAR, SHAR and SCHAR-r models for additional values of N ranging from 1 to 100, together with the 10% and 90% cross-sectional quantiles for the SCHAR-r forecasts. With the exception of QLIKE for $N = 2$, the median loss ratios for the SCHAR-r model are systematically below those of the other two models.

[22]Both of these loss functions may be formally justified for the purpose of volatility model forecast evaluation based on imperfect ex-post volatility proxies; see Patton (2011).

[23]The Supplemental Appendix reports the results from a series of additional forecasting models together with a more formal statistical comparison based on the Model Confidence Set (MCS) approach of Hansen, Lunde, and Nason (2011).

[24]Note that in the univariate case the positive and negative realized portfolio semicovariances coincide with the realized portfolio semivariances, so we do not consider the SCHAR model separately from the SHAR model.

Table 4: Portfolio Variance Forecasts

	MSE			QLIKE	
Model	Average	Ratio		Average	Ratio
			N = 1		
HAR	35.112	1.000		0.239	1.000
SHAR	34.981	0.997		0.238	0.998
			N = 10		
HAR	1.849	1.000		0.141	1.000
SHAR	1.671	0.966		0.139	0.986
SCHAR	1.643	0.955		0.210	1.318
SCHAR-r	1.567	0.908		0.139	0.979
			N = 100		
HAR	0.048	1.000		0.119	1.000
SHAR	0.045	0.935		0.115	0.957
SCHAR	0.045	0.976		0.236	1.495
SCHAR-r	0.041	0.862		0.111	0.925

Note: The table reports the loss for forecasting the portfolio variance for portfolios of size $N = 1, 10$ and 100 for each of the different forecasting models. The reported numbers are based on 500 randomly selected sets of stocks. The Average column provides the average loss over time and all sets of stocks. The Ratio column gives the time-average ratio over all sets of stocks relative to the HAR model.

Moreover, the gains from using the information in the realized semicovariances accrue relatively quickly as the number of stocks in the portfolio N increases, and for the QLIKE loss in particular appear to reach somewhat of a plateau for $N \approx 30$.[25]

3.4.2. A Time-Varying Parameter Interpretation

To help illuminate where the improvements in forecast accuracy are coming from, it is instructive to think about the forecasts that utilize the realized semicovariances as equivalent to the forecasts from a standard HAR-type model with time-varying parameters. To illustrate, consider the forecasts from a simple

[25]This is in line with the finding that the benefits to naïve diversification from the inclusion of randomly selected stocks in an all equity portfolio is close to exhausted at around 30 stocks; see, e.g., Campbell, Lettau, Malkiel, and Xu (2001).

Figure 5: Median Loss Ratios

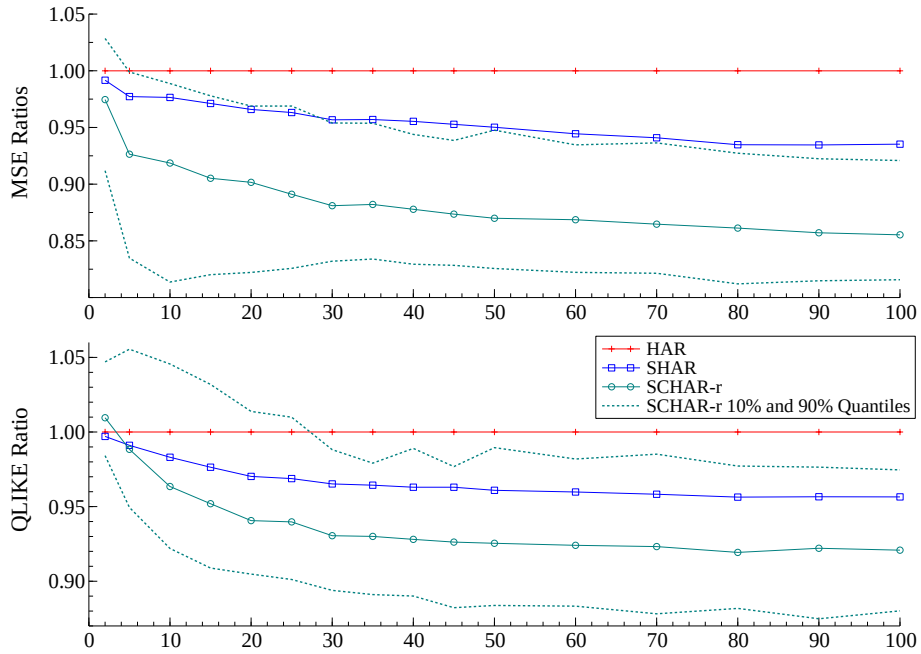

Note: The graph plots the median loss ratios as a function of the number of stocks in the portfolio, N. The ratio is calculated as the average loss of the models divided by the average loss of of the standard HAR, based on 500 random samples of N stocks.

SCHAR-type model based on the lagged daily variables only,

$$\begin{aligned} RV^p_{t+1|t} &= \phi_0 + \phi_{d,\mathcal{P}}\mathcal{P}^p_t + \phi_{d,\mathcal{N}}\mathcal{N}^p_t + \phi_{d,\mathcal{M}}\mathcal{M}^p_t \\ &= \phi_0 + \left(\phi_{d,\mathcal{P}}\frac{\mathcal{P}^p_t}{RV^p_t} + \phi_{d,\mathcal{N}}\frac{\mathcal{N}^p_t}{RV^p_t} + \phi_{d,\mathcal{M}}\frac{\mathcal{M}^p_t}{RV^p_t}\right) RV^p_t \\ &\equiv \phi_0 + \phi_{d,t}RV^p_t. \end{aligned}$$

As the last equation shows, even though the $\phi_{d,\mathcal{P}}$, $\phi_{d,\mathcal{N}}$ and $\phi_{d,\mathcal{M}}$ parameters in the original representation are all constant, this model may alternatively be interpreted as first-order autoregression for RV^p_{t+1} with a time-varying autoregressive parameter. This same idea obviously generalizes to the more complicated SCHAR-type forecasts, in which the parameters associated with the weekly and monthly lags in the implied HAR-type representations would be time-varying as well.

To this end, Figure 6 plots the implied daily, weekly and monthly HAR parameters for the SHAR and SCHAR-r variance forecasts for of a portfolio comprised of five stocks, or $N = 5$, averaged across 500 randomly selected such five-stock portfolios. In contrast to the out-of-sample forecasting results in Table 4, which

Figure 6: Implied HAR Parameters

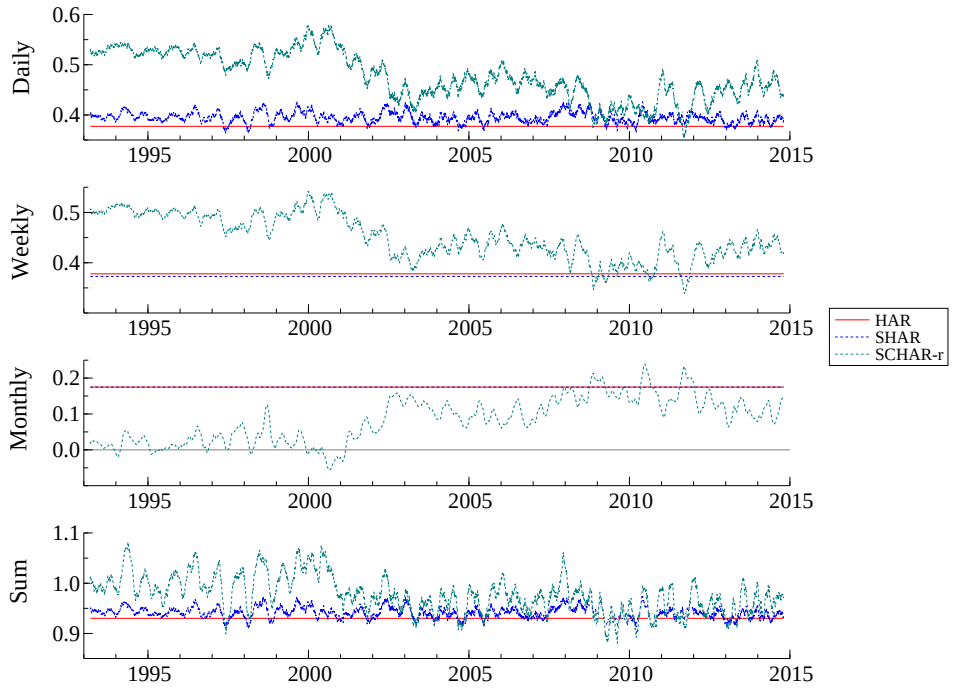

Note: The figure plots the implied HAR-type parameters for predicting the variance of a five-stock portfolio, averaged across 500 randomly selected portfolios. The models are estimated over the full sample period.

are based on a rolling estimation scheme, the figure plots the implied parameter estimates obtained over the full sample period.[26] In addition to the implied daily, weekly and monthly parameters, the last panel reports their sum as a measure of the overall persistence of the different models.

The parameters for the HAR model are constant by construction, with an average implied persistence of around 0.94. By comparison, the implied daily parameter estimates for the SHAR model vary slightly above the constant daily HAR parameter, while the constant weekly parameter for the SHAR model is slightly below that of the HAR model. As such, the overall persistence of the SHAR-based forecasts are generally very close to that of the standard HAR-based forecasts. By contrast, the implied time-varying daily and weekly parameter estimates for the SCHAR-r model far exceed those of the HAR model, especially

[26]Requiring observations to be available over the full sample reduces the number of stocks to 121. To avoid "contaminating" the results by a few influential outliers, we exclude any portfolios for which the maximum $\mathcal{P}_t^p/RV_t^p$, $\mathcal{P}_t^p/RV_t^p$ and $\mathcal{P}_t^p/RV_t^p$ ratios exceed ten, and further smooth the implied parameters using a $[t-25:t+25]$ moving average.

over the earlier part of the sample. On the other hand, the implied time-varying monthly parameters for the SCHAR-r model are typically less than for the HAR and SHAR models. Correspondingly, the sum of the three implied parameters for the SCHAR model are typically greater than for the other two models.[27] Thus, not only does the superior realized semicovariance-based forecasts respond more quickly to new information, the forecasts are typically also more persistent and slower to mean-revert.

4. Conclusion

We propose a new decomposition of the realized covariance matrix based on the signs of the underlying high-frequency returns. This generates four "realized semicovariance" matrices according to whether the returns were both positive, both negative, or had mixed signs. We derive the asymptotic distribution of the new measures under the standard assumption of a continuous multivariate semimartingale and the use of ever finer sampled high-frequency returns in their estimation. Relying on actual high-frequency data for a large cross-section of U.S. equities, we find that the realized semicovariances have distinctly different dynamic dependencies from the usual realized covariances, with the semicovariances based on discordant returns (i.e., returns of opposite signs) exhibiting the strongest memory. These differences in turn translate into superior forecast performance for models designed to "look inside" the covariance matrix and explicitly utilize the semicovariance measures.

Our work leaves open several interesting avenues for further research. One obvious direction entails the study of the asymptotic properties of the realized semicovariances in the presence of jumps, co-jumps, and dynamic leverage effects. Along these lines, it would be interesting to empirically investigate the economic drivers that cause the actual estimated semicovariance components to differ from their respective asymptotic limits. The small scale event-type study included in the paper provides a first step in that direction. All of the empirical results discussed in the paper are based on individual equities, effectively rendering the two discordant semicovariance components observational equivalent. It would be interesting to study the behavior of the realized semicovariances when one of the

[27] Even though the sum of the autoregressive coefficients for the SCHAR model occasionally exceeds unity, this does not necessarily imply non-stationary, as the temporal variation in the realized semicovariance measures may induce stationarity; see Conley, Hansen, Luttmer, and Scheinkman (1997) and Nielsen and Rahbek (2014) for a discussion of volatility induced stationarity.

assets is a market portfolio, or other systematic risk factor. This naturally links to earlier work on "asymmetric betas," and raises the tantalizing possibility of more accurate asset pricing models by decomposing conventional realized covariance-based betas into "realized semibetas." We leave all of these issues for future research.

5. References

Aït-Sahalia, Y., Xiu, D., 2015. Principal component analysis of high frequency data. Working paper, Princeton University.

Aït-Sahalia, Y., Xiu, D., 2016. Increased correlation among asset classes: Are volatility or jumps to blame, or both? Journal of Econometrics 194 (2), 205–219.

Aït-Sahalia, Y., Xiu, D., 2017. Using principal component analysis to estimate a high dimensional factor model with high-frequency data. Journal of Econometrics, Forthcoming.

Amaya, D., Christoffersen, P., Jacobs, K., Vasquez, A., 2015. Does realized skewness predict the cross-section of equity returns? Journal of Financial Economics 118 (1), 135–167.

Andersen, T. G., Bollerlsev, T., Diebold, F. X., Labys, P., 2003. Modeling and forecasting realized volatility. Econometrica 71 (2), 579–625.

Andersen, T. G., Bollerslev, T., Diebold, F. X., 2007. Roughing it up: Including jump components in the measurement, modeling, and forecasting of return volatility. Review of Economics and Statistics 89 (4), 701–720.

Andersen, T. G., Dobrev, D., Schaumburg, E., 2012. Jump-robust volatility estimation using nearest neighbor truncation. Journal of Econometrics 169 (1), 75–93.

Ang, A., Chen, J., 2002. Asymmetric correlations of equity portfolios. Journal of Financial Economics 63 (3), 443–494.

Barndorff-Nielsen, O. E., Graversen, S. E., Jacod, J., Podolskij, M., Shephard, N., 2006. A central limit theorem for realised power and bipower variations of continuous semimartingales. In "From Stochastic Analysis to Mathematical Finance, The Shiryaev Festschrift" (Edited by Y. Kabanov, R. Liptser and J. Stoyanov), Springer Verlag, 33–68.

Barndorff-Nielsen, O. E., Hansen, P. R., Lunde, A., Shephard, N., 2011. Multivariate realised kernels: Consistent positive semi-definite estimators of the covariation of equity prices with noise and non-synchronous trading. Journal of Econometrics 162 (2), 149–169.

Barndorff-Nielsen, O. E., Kinnebrock, S., Shephard, N., 2010. Measuring downside risk: realised semivariance. In "Volatility and Time Series Econometrics: Essays in Honor of Robert F. Engle" (Edited by T. Bollerslev, J. Russell and M. Watson), Oxford University Press, 117–136.

Barndorff-Nielsen, O. E., Shephard, N., 2004a. Econometric analysis of realized

covariation: High frequency based covariance, regression, and correlation in financial economics. Econometrica 72 (3), 885–925.

Barndorff-Nielsen, O. E., Shephard, N., 2004b. Power and bipower variation with stochastic volatility and jumps. Journal of Financial Econometrics 2 (1), 1–37.

Barndorff-Nielsen, O. E., Shephard, N., 2006. Econometrics of testing for jumps in financial economics using bipower variation. Journal of Financial Econometrics 4 (1), 1–30.

Bauwens, L., Laurent, S., Rombouts, J. V. K., 2006. Multivariate GARCH models: a survey. Journal of Applied Econometrics 21 (1), 79–109.

Bollerslev, T., Law, T., Tauchen, G., 2008. Risk, jumps and diversification. Journal of Econometrics 144 (1), 234–256.

Bollerslev, T., Patton, A. J., Quaedvlieg, R., 2016. Exploiting the errors: A simple approach for improved volatility forecasting. Journal of Econometrics 192 (1), 1–18.

Bollerslev, T., Todorov, V., 2011a. Estimation of jump tails. Econometrica 79 (6), 1727–1783.

Bollerslev, T., Todorov, V., 2011b. Tails, fears, and risk premia. Journal of Finance 66 (6), 2165–2211.

Campbell, J. Y., Lettau, M., Malkiel, B. G., Xu, Y., 2001. Have individual stocks become more volatility? An empirical exploration of idiosyncratic risk. Journal of Finance 56 (1), 1–43.

Caporin, M., Kolokolov, A., Renò, R., 2017. Systemic co-jumps. Journal of Financial Economics, Forthcoming.

Cappiello, L., Engle, R., Sheppard, K., 2006. Asymmetric dynamics in the correlations of global equity and bond returns. Journal of Financial Econometrics 4 (4), 537–572.

Conley, T., Hansen, L., Luttmer, E., Scheinkman, J., 1997. Short-term interest rates as subordinated diffusions. Review of Financial Studies 10 (3), 525–577.

Corsi, F., 2009. A simple approximate long-memory model of realized volatility. Journal of Financial Econometrics 7 (2), 174–196.

Corsi, F., Pirino, D., Renò, R., 2010. Threshold bipower variation and the impact of jumps on volatility forecasting. Journal of Econometrics 159 (2), 276–288.

Das, S. R., Uppal, R., 2004. Systemic risk and international portfolio choice. Journal of Finance 59 (6), 2809–2834.

Doornik, J., 2009. Object-oriented Matrix Programming Using Ox. Timberlake Consultants Press.

Duffie, D., Pan, J., Singleton, K., 2000. Transform analysis and asset pricing for

affine jump-diffusions. Econometrica 68 (6), 1343–1376.

Elton, E. J., Gruber, M. J., 1973. Estimating the dependence structure of share prices – Implications for portfolio selection. Journal of Finance 28 (5), 1203–1232.

Engle, R. F., 2002. Dynamic conditional correlation: A simple class of multivariate generalized autoregressive conditional heteroskedasticity models. Journal of Business and Economic Statistics 20 (2), 339–350.

Epps, T. W., 1979. Comovements in stock prices in the very short run. Journal of the American Statistical Association 74 (366a), 291–298.

Fan, J., Li, Y., Yu, K., 2012. Vast volatility matrix estimation using high-frequency data for portfolio selection. Journal of the American Statistical Association 107 (497), 412–428.

Fishburn, P. C., 1977. Mean-risk analysis with risk associated with below-target returns. American Economic Review 67 (2), 116–126.

Goncalves, S., Meddahi, N., 2009. Bootstrapping realized volatility. Econometrica 77 (1), 283–306.

Hansen, P. R., Huang, Z., Shek, H. H., 2012. Realized garch: a joint model for returns and realized measures of volatility. Journal of Applied Econometrics 27 (6), 877–906.

Hansen, P. R., Lunde, A., 2006. Realized variance and market microstructure noise. Journal of Business and Economic Statistics 24 (2), 127–161.

Hansen, P. R., Lunde, A., 2014. Estimating the persistence and the autocorrelation function of a time series that is measured with error. Econometric Theory 30 (1), 60–93.

Hansen, P. R., Lunde, A., Nason, J. M., 2011. The model confidence set. Econometrica 79 (2), 453–497.

Hautsch, N., Kyj, L. M., Malec, P., 2015. Do high-frequency data improve high-dimensional portfolio allocations? Journal of Applied Econometrics 30 (2), 263–290.

Hogan, W. W., Warren, J. M., 1972. Computation of the efficient boundary in the E-S portfolio selection model. Journal of Financial and Quantitative Analysis 7 (4), 1881–1896.

Hogan, W. W., Warren, J. M., 1974. Toward the development of an equilibrium capital-market model based on semivariance. Journal of Financial and Quantitative Analysis 9 (1), 1–11.

Hong, Y., Tu, J., Zhou, G., 2007. Asymmetries in stock returns: Statistical tests and economic interpretation. Review of Financial Studies 20 (5), 1547–1581.

Jacod, J., Li, Y., Zheng, X., 2017. Statistical properties of microstructure noise. Econometrica 85 (4), 1133–1174.

Jacod, J., Todorov, V., 2009. Testing for common arrivals of jumps for discretely observed multidimensional processes. Annals of Statistics 37 (4), 1792–1838.

Kendall, M. G., 1953. The analysis of economic time-series – Part I: Prices. Journal of the Royal Statistical Society, Series A 116 (1), 11–34.

Kinnebrock, S., Podolskij, M., 2008. A note on the central limit theorem for bipower variation of general functions. Stochastic processes and their applications 118 (6), 1056–1070.

Kroner, K. F., Ng, V. K., 1998. Modeling asymmetric comovements of asset returns. Review of Financial Studies 11 (4), 817–844.

Lahaye, J., Laurent, S., Neely, C. J., 2011. Jumps, cojumps and macro announcements. Journal of Applied Econometrics 26 (6), 893–921.

Lee, S. S., 2012. Jumps and information flow in financial markets. Review of Financial Studies 25 (2), 439–479.

Lee, S. S., Mykland, P. A., 2008. Jumps in financial markets: A new nonparametric test and jump dynamics. Review of Financial Studies 21 (6), 2535–2563.

Li, J., Todorov, V., Tauchen, G., 2017. Jump regressions. Econometrica 85 (1), 173–195.

Longin, F., Solnik, B., 2001. Extreme correlation of international equity markets. Journal of Finance 56 (2), 649–676.

Mancini, C., 2009. Non-parametric threshold estimation for models with stochastic diffusion coefficient and jumps. Scandinavian Journal of Statistics 36 (2), 270–296.

Mancini, C., Gobbi, F., 2012. Identifying the brownian covariation from the cojumps given discrete observations. Econometric Theory 28 (2), 249–273.

Mao, J. C. T., 1970. Survey of capital budgeting: Theory and practice. Journal of Finance 25 (2), 349–360.

Markowitz, H. M., 1959. Portfolio Selection. Wiley.

Mykland, P. A., Zhang, L., 2009. Inference for continuous semimartingale observed at high frequency. Econometrica 77 (5), 1403–1445.

Mykland, P. A., Zhang, L., 2017. Assessment of uncertainty in high frequency data: The observed asymptotic variance. Econometrica 85, 197–231.

Neuberger, A., 2012. Realized skewness. Review of Financial Studies 25 (11), 3423–3455.

Nielsen, H. B., Rahbek, A., 2014. Unit root vector autoregression with volatility induced stationarity. Journal of Empirical Finance 29, 144–167.

Noureldin, D., Shephard, N., Sheppard, K., 2012. Multivariate high-frequency-based volatility (heavy) models. Journal of Applied Econometrics 27 (6), 907–933.

Patton, A. J., 2004. On the out-of-sample importance of skewness and asymmetric dependence for asset allocation. Journal of Financial Econometrics 2 (1), 130–168.

Patton, A. J., 2011. Volatility forecast comparison using imperfect volatility proxies. Journal of Econometrics 160 (1), 246–256.

Patton, A. J., Sheppard, K., 2015. Good volatility, bad volatility: Signed jumps and the persistence of volatility. Review of Economics and Statistics 97 (3), 683–697.

Poon, S.-H., Rockinger, M., Tawn, J., 2004. Extreme value dependence in financial markets: Diagnostics, models, and financial implications. Review of Financial Studies 17 (2), 581–610.

Tjøsthem, D., Hufthammer, K. O., 2013. Local gaussian correlation: A new measure of dependence. Journal of Econometrics 172 (1), 33–48.

Zellner, A., 1992. Presidential address: Statistics, science and public policy. Journal of the American Statistical Association 87 (417), 1–6.

Appendix A. Proofs of Propositions

To simplify the exposition, let $\mathbf{U} = [U^{(1)}, U^{(2)}]$ denote a bivariate standard normal random variable, f be a real-valued function on $\mathbb{R}^2$, and define

$$\rho_{\boldsymbol{\sigma}}(f) \equiv \mathbb{E}[f(\boldsymbol{\sigma}\mathbf{U})], \tag{A.1}$$

$$\rho_{\boldsymbol{\sigma}}^{(k)}(f) \equiv \mathbb{E}[f(\boldsymbol{\sigma}\mathbf{U})U^{(k)}], \tag{A.2}$$

for $k = 1, 2$.

Proof of Proposition 1: Given the assumptions in equations (12) and (14), coupled with the fact that the 8×1 vector function $\mathbf{g}$ defined in equation (11) is continuously differentiable and of polynomial growth, the limit of $\mathbf{V}^{(m)}$ can be derived using the theory of Kinnebrock and Podolskij (2008). In particular, applying their Theorem 1 to $\mathbf{V}^{(m)}$ in equation (11) it follows that,

$$\mathbf{V}^{(m)} \xrightarrow{P} \mathbf{V} = \int_0^1 \rho_{\boldsymbol{\sigma}_u}(\mathbf{g})du. \tag{A.3}$$

Let $\mathbf{Z} = \boldsymbol{\sigma}_u\mathbf{U}$ be bivariate normal with mean zero and covariance matrix,

$$\boldsymbol{\sigma}_u\boldsymbol{\sigma}_u' = \begin{bmatrix} \sigma_{u,1}^2 & \rho_u \\ \rho_u & \sigma_{u,2}^2 \end{bmatrix}, \tag{A.4}$$

we obtain the following expressions for $\rho_{\boldsymbol{\sigma}_u}(g_i)$, for $i = 1, 2, ..., 8$,

$$\rho_{\boldsymbol{\sigma}_u}(g_1) = \rho_{\boldsymbol{\sigma}_u}(g_2) = \mathbb{E}\left[Z_1^2 I_{\{Z_1 \geq 0\}}\right] = \frac{\sigma_{u,1}^2}{2}$$

$$\rho_{\boldsymbol{\sigma}_u}(g_3) = \rho_{\boldsymbol{\sigma}_u}(g_4) = \mathbb{E}\left[Z_2^2 I_{\{Z_2 \geq 0\}}\right] = \frac{\sigma_{u,2}^2}{2}$$

$$\rho_{\boldsymbol{\sigma}_u}(g_5) = \rho_{\boldsymbol{\sigma}_u}(g_6) = \mathbb{E}\left[Z_1 Z_2 I_{\{Z_1 \geq 0, Z_2 \geq 0\}}\right] = \frac{\sigma_{u,1}\sigma_{u,2}\left(\rho_u \arccos(-\rho_u) + \sqrt{1-\rho_u^2}\right)}{2\pi}$$

$$\rho_{\boldsymbol{\sigma}_u}(g_7) = \rho_{\boldsymbol{\sigma}_u}(g_8) = \mathbb{E}\left[Z_1 Z_2 I_{\{Z_1 \geq 0, Z_2 < 0\}}\right] = \frac{\sigma_{u,1}\sigma_{u,2}\left(\rho_u \arccos\rho_u - \sqrt{1-\rho_u^2}\right)}{2\pi},$$

which completes the proof. □

Proof of Proposition 2: Under Assumption (14), Theorem 2 of Kinnebrock and Podolskij (2008) implies the following CLT for $\mathbf{V}^{(m)}$,

$$\sqrt{m}(\mathbf{V}^{(m)} - \mathbf{V}) \xrightarrow{\mathcal{D}_{st}} \int_0^1 \boldsymbol{\alpha}_u d\mathbf{W}_u + \int_0^1 \boldsymbol{\beta}_u d\tilde{\mathbf{W}}_u, \tag{A.5}$$

where $\xrightarrow{\mathcal{D}_{st}}$ denotes stable convergence, $\boldsymbol{\alpha}_u$, $\boldsymbol{\beta}_u$ are 8×2-dimensional processes, $\tilde{\mathbf{W}}$ is a two-dimensional Brownian motion independent of the $\mathbf{W}$ and $\mathbf{W}^*$ Brownian motions in (12) and (14). Elementwise, $\boldsymbol{\alpha}_u$ and $\boldsymbol{\beta}_u$ are defined as follows,

$$\alpha_u^{(a,b)} = \rho_{\boldsymbol{\sigma}_u}^{(b)}(g_a), \tag{A.6}$$

with

$$\boldsymbol{\beta}_u \boldsymbol{\beta}_u' = \mathbf{A}_u - \boldsymbol{\alpha}_u \boldsymbol{\alpha}_u', \tag{A.7}$$

where $\mathbf{A}_u$ is the 8×8 matrix with elements,

$$A_u^{(a,b)} = \rho_{\boldsymbol{\sigma}_u}(g_a g_b) - \rho_{\boldsymbol{\sigma}_u}(g_a)\rho_{\boldsymbol{\sigma}_u}(g_b). \tag{A.8}$$

The following equations provide the requisite expressions for the elements of $\rho_{\boldsymbol{\sigma}_u}$,

$$\begin{aligned}
\rho_{\boldsymbol{\sigma}_u}((g_1)^2) &= \rho_{\boldsymbol{\sigma}_u}((g_2)^2) = \frac{3\sigma_{u,1}^4}{2} \\
\rho_{\boldsymbol{\sigma}_u}((g_3)^2) &= \rho_{\boldsymbol{\sigma}_u}((g_4)^2) = \frac{3\sigma_{u,2}^4}{2} \\
\rho_{\boldsymbol{\sigma}_u}((g_5)^2) &= \rho_{\boldsymbol{\sigma}_u}((g_6)^2) = \frac{\sigma_{u,1}^2\sigma_{u,2}^2}{2\pi}\left[(1+2\rho_u^2)\arccos(-\rho_u) + 3\rho_u\sqrt{1-\rho_u^2}\right] \\
\rho_{\boldsymbol{\sigma}_u}((g_7)^2) &= \rho_{\boldsymbol{\sigma}_u}((g_8)^2) = \frac{\sigma_{u,1}^2\sigma_{u,2}^2}{2\pi}\left[(1+2\rho_u^2)\arccos(\rho_u) - 3\rho_u\sqrt{1-\rho_u^2}\right]
\end{aligned}$$

$$\begin{aligned}
\rho_{\boldsymbol{\sigma}_u}(g_1 g_3) &= \rho_{\boldsymbol{\sigma}_u}(g_2 g_4) = \rho_{\boldsymbol{\sigma}_u}((g_5)^2) \\
\rho_{\boldsymbol{\sigma}_u}(g_1 g_4) &= \rho_{\boldsymbol{\sigma}_u}(g_2 g_3) = \rho_{\boldsymbol{\sigma}_u}((g_7)^2) \\
\rho_{\boldsymbol{\sigma}_u}(g_1 g_5) &= \rho_{\boldsymbol{\sigma}_u}(g_2 g_6) = \frac{\sigma_{u,1}^3\sigma_{u,2}}{2\pi}\left[3\rho_u\arccos(-\rho_u) + (2+\rho_u^2)\sqrt{1-\rho_u^2}\right] \\
\rho_{\boldsymbol{\sigma}_u}(g_1 g_7) &= \rho_{\boldsymbol{\sigma}_u}(g_2 g_8) = \frac{\sigma_{u,1}^3\sigma_{u,2}}{2\pi}\left[3\rho_u\arccos(\rho_u) - (2+\rho_u^2)\sqrt{1-\rho_u^2}\right] \\
\rho_{\boldsymbol{\sigma}_u}(g_3 g_5) &= \rho_{\boldsymbol{\sigma}_u}(g_4 g_6) = \frac{\sigma_{u,1}\sigma_{u,2}^3}{2\pi}\left[3\rho_u\arccos(-\rho_u) + (2+\rho_u^2)\sqrt{1-\rho_u^2}\right] \\
\rho_{\boldsymbol{\sigma}_u}(g_3 g_8) &= \rho_{\boldsymbol{\sigma}_u}(g_4 g_7) = \frac{\sigma_{u,1}\sigma_{u,2}^3}{2\pi}\left[3\rho_u\arccos(\rho_u) - (2+\rho_u^2)\sqrt{1-\rho_u^2}\right],
\end{aligned}$$

with all other elements $\rho_{\boldsymbol{\sigma}_u}(g_a g_b) = 0$, as the relevant events are mutually exclusive. Finally, the elements of $\rho^{(k)}_{\boldsymbol{\sigma}_u}$ are given by,

$$\begin{aligned}
\rho^{(1)}_{\boldsymbol{\sigma}_u}(g_1) = -\rho^{(1)}_{\boldsymbol{\sigma}_u}(g_2) &= \frac{2\sigma^2_{u,1}}{\sqrt{2\pi}} \\
\rho^{(1)}_{\boldsymbol{\sigma}_u}(g_3) = -\rho^{(1)}_{\boldsymbol{\sigma}_u}(g_4) &= \frac{2\rho_u\sigma^2_{u,2}}{\sqrt{2\pi}} \\
\rho^{(2)}_{\boldsymbol{\sigma}_u}(g_1) = -\rho^{(2)}_{\boldsymbol{\sigma}_u}(g_2) &= \frac{2\rho_u\sigma^2_{u,1}}{\sqrt{2\pi}} \\
\rho^{(2)}_{\boldsymbol{\sigma}_u}(g_3) = -\rho^{(2)}_{\boldsymbol{\sigma}_u}(g_4) &= \frac{2\sigma^2_{u,2}}{\sqrt{2\pi}} \\
\rho^{(1)}_{\boldsymbol{\sigma}_u}(g_5) = -\rho^{(1)}_{\boldsymbol{\sigma}_u}(g_6) = \rho^{(2)}_{\boldsymbol{\sigma}_u}(g_5) = -\rho^{(2)}_{\boldsymbol{\sigma}_u}(g_6) &= \frac{\sigma_{u,1}\sigma_{u,2}(\rho_u+1)^2}{2\sqrt{2\pi}} \\
\rho^{(1)}_{\boldsymbol{\sigma}_u}(g_7) = -\rho^{(1)}_{\boldsymbol{\sigma}_u}(g_8) = -\rho^{(2)}_{\boldsymbol{\sigma}_u}(g_7) = \rho^{(2)}_{\boldsymbol{\sigma}_u}(g_8) &= -\frac{\sigma_{u,1}\sigma_{u,2}(\rho_u-1)^2}{2\sqrt{2\pi}},
\end{aligned}$$

which completes the proof. □

Proof of Proposition 3: The consistency of $\boldsymbol{\Pi}^{(m)}$ for $\boldsymbol{\Pi}$, and in turn the asymptotic distribution of the normalized estimator, follows directly from Corollary 1 in Kinnebrock and Podolskij (2008). □